Biomolecular Corona Associated with Nanostructures: The Potentially Disruptive Role of Raman Microscopy

ADVANCED MATERIALS TECHNOLOGIES
www.advmattechnol.de

Biomolecular Corona Associated with Nanostructures: The Potentially Disruptive Role of Raman Microscopy

Matteo Battaglini, Melike Belenli Gümüş,* and Gianni Ciofani**

When nanostructures and other materials are exposed to biological fluids, they are immediately covered by a layer of biological molecules, which is typically referred to as a "biomolecular corona" (BC). This represents the first component of a material that interacts with biological systems, so characterizing the composition and the dynamic evolution of BC is essential for predicting the interactions of materials and living organisms. This review provides an analysis of current BC characterization techniques, with particular attention to nanostructures involved in biomedical applications. The influence on cell–nanostructure interactions is assessed and the advantages and limitations of each technique are discussed and compared. An in-depth analysis of Raman microscopy, a relatively unexploited tool with great potential in the characterization of BC, is then conducted. Raman microscopy can be used to analyze a vast amount of specimens without the need for staining, and can provide analysis on a spatial scale of hundreds of nanometers: it may thus represent a potentially disruptive tool for the characterization of BC, as it overcomes many of the limitations posed by current techniques.

1. Introduction

The potential of using nanomaterials for the treatment of diseases has increased in recent years. Scientific research has focused on understanding how biological molecules interact with different types of nanomaterials that can be used in nanomedicine and drug delivery applications. The formation of so-called "coronas" on the surfaces of nanomaterials after they are introduced into a biological system must be considered when investigating the use of nanomaterials within living organisms. When a nanoparticle (NP) encounters biological molecules such as proteins, lipids, nucleic acids, or polysaccharides, it tends to adsorb these molecules on its surface due to electrostatic, hydrophobic, or other forms of interactions between the molecules and the surface of the NP.[1–4] Depending on their abundance and affinity, proteins and other molecules may form a hard corona that consists of tightly bounded proteins on the surface, or a soft corona, which indicates a second layer of proteins that are loosely attached to the proteins of the hard corona.[4] The composition of the soft corona changes over time according to the environmental conditions, and so the biological identity of nanostructures is usually, but not always, determined by the hard corona. This can be both advantageous and disadvantageous to the application of NPs. Some studies have focused on preventing biomolecular corona (BC) formation, as this may change the size and surface properties, hinder modifications on the surface, and cause the rapid detection and clearance of NPs by the immune system.[5,6] However, BCs can be exploited or even altered, in order to be made beneficial for targeting purposes as they can enable specific cells to more easily recognize NPs and may lead to a reduction in their toxicity.[7,8]

A wide range of techniques have been used in BC studies, such as dynamic light scattering (DLS),[9] sodium dodecyl sulfate-polyacrylamide gel electrophoresis (SDS-PAGE), mass spectrometry (MS)-based approaches,[10–21] UV/vis spectroscopy, Fourier-transform infrared spectroscopy (FTIR),[22] atomic force microscopy (AFM),[23] scanning electron microscopy (SEM),[24–27] transmission electronic microscopy (TEM),[23] and circular dichroism spectroscopy (CD).[28] Various information (size, surface properties, morphology, structure, etc.) about BCs can be obtained through these methods. Many techniques have been applied in BC studies, which can be divided into microscopy-based approaches that use direct imaging of the sample, and indirect techniques. Microscopy techniques can provide information about corona composition and shape with a spatial resolution up to the dimension scale of single protein molecules, but they are limited by the requirement for staining or extensive sample preparation. Indirect techniques can provide extensive information about BC–nanostructure interactions and properties, but typically have a limited resolution and so cannot analyze the BC at the level of single nanostructures. Other emerging

M. Battaglini, M. Belenli Gümüş, G. Ciofani
Italian Institute of Technology
Smart Bio-Interfaces
Viale Rinaldo Piaggio 34, Pontedera, Pisa 56025, Italy
E-mail: matteo.battaglini@iit.it; melike.belenli@iit.it; gianni.ciofani@iit.it
M. Belenli Gümüş
Scuola Superiore Sant'Anna
The Biorobotics Institute
Viale Rinaldo Piaggio 34, Pontedera, Pisa 56025, Italy
The ORCID identification number(s) for the author(s) of this article can be found under https://doi.org/10.1002/admt.202100660.

DOI: 10.1002/admt.202100660

techniques based on the phenomenon of Raman scattering can give invaluable information about interactions between NPs and biomolecules and thus have great potential in BC studies. Raman phenomenon explains how light is inelastically scattered due to the vibrational modes of molecules, and how it can be used to determine the type of bonds in a sample.[29] Many techniques, such as Raman spectroscopy, surface-enhanced Raman spectroscopy (SERS), and confocal Raman microscopy (CRM) have been developed based on this phenomenon. These techniques can provide information directly about the nanostructure–biomolecule interface,[30] and thus can be useful in understanding the conformation of molecules on the surface of NPs and the mechanisms of the interactions.[31,32] They can also be used for visualizing the sample without any labeling requirement.[33] We suggest that Raman spectroscopy, and in particular Raman microscopy, represents a technological bridge between direct microscopy-based analysis and indirect measurements of the BC, and can provide a vast amount of information about BC composition and properties with a high spatial resolution, without the need for staining procedures.

In the first part of this review, we examine the biomolecular corona in terms of its characteristics, formation, and effect on the functionality of NPs. Analytical methods that have been widely used in BC research are discussed in the second part, with examples from recent studies. In the final part, Raman spectroscopy and related techniques are briefly introduced, and the contribution of these methods to the interaction of nanoparticle–biomolecule research is discussed in detail, emphasizing their extensive potential in BC investigations.

2. Biomolecular Corona: Significance, Characteristics, and Exploitation

In this section, we discuss the importance of BC. We divide our analysis into three main parts:

1) The impact of BC: how its presence affects the properties and functionality of nanostructures in general;
2) The characteristics of BC: the parameters that can affect BC formation, composition, and BC-induced biological responses;
3) Opportunities for exploiting BC formation to improve nanostructure properties.

These topics are discussed in detail through the use of examples of current BC studies in the literature.

2.1. The Impact of the Biomolecular Corona

Understanding how BCs can affect nanostructure properties and activities is the main focus of BC studies, as this can result in nanodevices having unexpected and undesired effects when exposed to biological media. One common effect of the formation of BCs on nanostructure surfaces is an increase in the aggregation of the nanostructures themselves and a reduction in stability when in solution. For example, Dominguez-Medina et al. analyzed this phenomenon on gold nanorods exposed to bovine serum albumin (BSA) and found that BSA was able to bind to the surface of the nanorods, forming a BC. The bounded BSA was then subjected to structural rearrangement and unfolding, which led to cross-interactions between BSA molecules and thus particle aggregation.[5] Interestingly, different proteins can have different effects on particles stability when associated with their surface, and may even increase the colloidal stability of the nanostructures themselves. For example, when gold NPs (AuNPs) are exposed to immunoglobulin G (IgG), fibrinogen (FBG), apolipoprotein A1 (ApoA1), or human serum albumin (HSA), they can have different effects on the stability of the nanostructures, and this effect is concentration-dependent (a higher protein/particles ratio leads to higher colloidal stability).[34] The effect of BC on nanostructures stability is not only dependent on the molecular composition of the BC itself, but can also be affected by complex interactions between the BC and the biological environment. For example, the exposure of the BC–particle complex to different pH levels may lead to aggregation due to the structural change occurring at the level of the protein molecules present in the BC. This effect is particularly evident when these protein molecules are exposed to pH levels that are very different from that of their isoelectric point.[35] The presence of BC can greatly affect the biocompatibility of nanostructures, leading to adverse reactions from both cells and living organisms. For example, it has been shown that the presence of growth factor β1 (TGF-β1) in the BC formed around silica NPs can enhance the ability of these particles to induce lung fibrosis in mice.[10] The adverse effects from the association of BC with nanostructures are typically caused by a change in the interaction levels between nanostructures–BC complexes and immune cells, rather than bare nanostructures. For example, the interactions of silver NPs (AgNPs) exposed to different protein sources were found to significantly differ in macrophages, depending on their derived protein coronas (PCs).[36] This process of interaction between BC–nanostructures and immune cells can be extremely complex and involves a wide variety of molecules in the BC and receptors at the cellular level, as demonstrated by Lara et al., who found that fluorescently labeled SiO_2 NPs exposed to biological media can interact with a macrophage receptor with collagenous structure (MARCO) in a form that does not demonstrate any competition phenomena with other known ligands in MARCO such as LPS.[37] In addition, the interaction of gold nanostructures with the immune system has been demonstrated to be linked to the formation of BC. Gold nanorods with different surface chemistries can change their interactions with macrophage depending on the composition of their BC, leading to more or less interleukin 1β being released.[12] The source of molecules from which the BC is derived can be an important parameter in determining the immune response caused by BC–particle complexes, which has been demonstrated by administrating Gd@C82(OH)22 NPs exposed to human lung squamous cell carcinoma. When exposed to carcinoma cells, these nanostructures acquired a BC enriched in complement 1q, causing an enhanced immune response compared to BC free nanostructures.[38] The immune response to BC–nanostructure complexes is not only affected by the molecular composition of the BC itself, but also by the molecular structure of the moieties associated with the nanostructures themselves. For example, the post-translational modification of protein has been proven to be a major factor in determining the interaction between

nanostructures and the immune system, as in silica nanostructure BC, where the presence of glycosylation processes has been shown to affect cell–particle interactions and to induce an inflammatory response.[2] Hemocompatibility can also be affected by the presence of BC, leading to a change in the interaction between nanostructures and blood components.[39,40] Blood interaction with BC–protein complexes can be made more complex by the interaction with anticoagulants. For example, it has been shown that the BC formed on the surface of poly(lactic acid) (PLA), polycaprolactone (PCL), silica, and a polystyrene vascular targeted carrier when exposed to both serum and whole blood is significantly affected by the presence of heparin, demonstrating an increase in their vascular targeting and adhesion efficiency.[41] A major concern related to the phenomena of BC formation is the effect that a BC can have upon the targeting efficiency of nanostructures, which is generally related to the "shielding" effect that the molecules of BC can have on the targeting molecules associated with the nanostructures.[11] Cellular internalization of nanostructures is a biological phenomenon that is probably affected by the presence of BC to a great extent. For example, Digiacomo et al. demonstrated how the formation of BC on the surface of multicomponent lipid NPs can shift the pathway internalization of Hela cell particles from micropinocytosis to clathrin-dependent endocytosis.[42] Other examples of nanostructure–cell interaction affected by BCs include bacterial magnetosomes.[43] Silica NPs showed an increase in their uptake by macrophages when preincubated with gamma globulins[26] and gold nanostructures.[44] The effect of BCs on nanostructures cell interaction is not only determined by BC molecular composition. For example, particles of the same size and shape associated with the same proteins can have different interactions with biological systems. This apparently paradoxical result has been explained by the effect of surface charge. Polystyrene nanostructures with anionic or cationic are both covered by BSA, but the protein molecules on the surface of the nanostructures can be in their native state or denatured depending on the particle charge, thus determining the biological behavior of the nanostructures.[45] However, BC formation on the surface of nanostructures is not always detrimental to their targeting efficiency. For example, it has been shown that if stealth pegylated functionalized liposome evolve a BC after exposure to in vivo conditions, the BC is very sparse and does not affect the targeting efficiency of antibody functionalized nanostructures.[46] Oddly, the targeting efficiency of nanodevices can be preserved even in cases where the formation of BCs causes major changes in nanostructure properties and may go as far as to change the particle surface potential. The study of Zhao et al. demonstrated this, in which electrically positive magnetic NPs did not lose their ability to target cancer cells, even after the surface charge potential shift caused by the exposure of these particles to proteins occurred. As the authors discussed, this may be due to an asymmetrical distribution of charge on the surface of NPs, with both positive and negative zones caused by the inhomogeneous binding of proteins.[19] As discussed in detail in the following paragraphs, the formation of BC can be used as a tool for improving the targeting properties of particles.[11] BCs can have effects on more specific nanostructure activities, such as the exposure to biological media of nanoflares based on AuNPs used for the detection of oligonucleotides. This has been demonstrated to cause a significant reduction in the signals generated by nanoflares compared to the signal efficiency of BC-free nanostructures.[47] Other examples include the effect of BC on the results of immunoassay[48] and the reduction of the activities of antibacterial nanostructures.[49,50] Nanodevices used as a transfection vector are a class of nanostructure that are significantly affected by the formation of BCs. Several studies demonstrate how the exposure of these nanostructures to biological media can drastically reduce their transfection efficiency. For example, a model has been proposed that describes the BC formed on the surface of lipoplexes as being the principal cause of the shift between caveolae-mediated endocytosis to micropinocytosis uptake. This shift has been shown to cause an accumulation of lipoplexes in the lysosomal degradative compartment, with a resulting reduction of nanostructures transfection efficiency.[51] Similar results have been obtained for polyplexes used for cellular transfection, where nanostructure–BC complexes demonstrated an increase in lysosomal localization compared to BC-free nanostructures, and a reduction of transfection efficiency.[52] In another example, graphene oxide nanoflakes coated with cationic lipids and loaded with DNA showed a significant reduction in their transfection abilities, due to the formation of BC on their surfaces.[53] It appears that the inner structure of lipid NPs used as transfection agents is closely linked to their ability to form BC and their transfection efficiency. For example, Betker et al. examined how BC formation on the surface of DOTAp base lipoplexes was affected both by the lipidic composition of the nanostructures (in particular in terms of cholesterol) and by the presence of poly ethylene glycol (PEG). Interestingly, the increase in cholesterol levels in the composition of DOTAp lipoplexes can reduce the formation of BCs and counterintuitively, PEG can increase the number of proteins attached to the surfaces of DOTAp lipoplexes. These changes in BC composition were linked to the transfection efficiency of these nanostructures.[54] Not only is the BC formation process affected by the lipidic composition of lipid base nanostructures, but also the lipidic composition itself can be affected by the formation of BC. For example, BC formation was able to change the lipidic bilayer structure of PEGylated cationic liposomes (CLs), leading to particle aggregation.[55] BC formation is not a phenomenon specific to 1D nanostructures, but also occurs in bidimensional nanostructures like nanosheets, which can be associated with a BC on exposure to biological media, leading to the potential stimulation of inflammatory and immunogenic responses.[6] For example, graphene oxide nanosheets exposed to plasma that is derived from various subjects affected by different conditions evolved BC specific to the serum source, which has a major impact on the biocompatibility of nanostructures.[56] Finally, a BC is not a phenomenon restricted to artificially produced nanostructures, and even endogenous molecules involved in pivotal physiological processes can aggregate to form nanostructures associated with BCs. For example, it has been shown that amyloid-β (Aβ) plaques can present an associated BC, and even more interestingly, different forms of amyloids present different associated proteins.[57] Another example is the BC formed on the surface of islet amyloid polypeptide (IAPP). The aggregation of IAPP is commonly associated with beta-cell death in type-2 diabetes (T2D). A BC analysis suggested that the absorption of proteins on the surface of IAPP aggregates is a key feature in the

aggregation of IAPP and in terms of its toxicity.[58] Similarly, human IAPP fibrils have been associated with BCs.[59] BCs can also be formed on the surface of viruses, such as the herpes simplex virus type 1 (HSV-1), which has been shown to recruit a complex BC on its surface after exposure to biological media. This virus-associated BC can significantly affect virus infectivity and immune response and moreover it has been demonstrated that HSV-1 can recruit amyloidogenic peptides on its surface, catalyzing the aggregation of amyloid β-peptide (Aβ42), which is a major component of amyloid plaques in Alzheimer's disease (AD) and represent a common hallmark of AD.[60] A summary of BC composition and its impact upon nanostructures properties is provided in **Figure 1**.

2.2. The Characteristics of Biomolecular Coronas and Parameters Affecting Their Formation and Evolution

When coming into contact with biological media, nanostructures can become covered by numerous molecules, which make up the BC. The BC associated with nanostructures has been shown to form as quickly as 10 min after the nanostructures are exposed to the biological media.[61] A BC is typically classified based on its level and proximity of interaction with the associated nanostructures surface. Molecules associated directly with the nanostructure surface form what is called a "hard corona," while other molecules not directly attached to the nanostructure surface form a heterogeneous and loosely organized layer of molecules, commonly called a "soft corona." As mentioned previously, BC is not only composed of proteins but can also include other biological molecules. For example, the concept of "lipid corona" has emerged in recent years to describe the lipids associated with nanostructures. Liposomal NPs, after their exposure to biological media, have been associated with at least 166 different lipidic molecules including phospholipids, steroids, carnitines, fatty alcohols, diglycerides, and fatty acids. The main explanation for this abundance of lipids on the surface of these nanostructures is the interaction between the nanostructures themselves and proteins associated with lipids.[62] It appears that apolipoprotein can disintegrate upon interaction with certain nanostructures, with the subsequent adsorption of lipid on the surface of the particles.[63] Other molecules that can be associated with nanostructures surface include small metabolites (<1000 kDa), which can constitute the "metabolic corona."[64] Hard corona and soft corona can be formed by different molecules,[65] but they should not be conceived as completely separate objects. For example, AuNPs exposed to complete media are at first covered by a loosely attached corona that evolves into an irreversible bounded corona over time.[66] To better describe the molecular interactions governing the BC formation and evolution, the concept of "corona interactome" has recently been introduced, which refers to the progressive build-up of BC due to protein–protein and other molecular interactions involving on one side the moieties in the BC and on the other the molecules in the surrounding environment.[67] BC characteristics, in terms of molecular composition, shape, size, electric charge, and time-dependent evolution, can be divided into parameters they affect. First, they influence the intrinsic properties of the nanostructures associated with the BC such as size, shape porosity, chemistry, surface charge, and surface functionalization, and second, the extrinsic parameters associated with the biological environment surrounding the BC–nanostructure complexes, such as the molecular composition of the biological media, pH, temperature, or the presence of dynamic conditions. Particle size and shape have been identified as important parameters in determining the formation and evolution of BCs. For example, AuNPs with different sizes and different shapes have been shown to form different BCs, once exposed to biological media.[68–70] Smaller particles tend to associate with a larger amount of proteins and other molecules, due to an increased ratio of surface area/volume compared to bigger particles. Porosity can also affect the composition of BCs, with a high porosity nanostructure attracting a higher percentage of low molecular weight (MW) molecules, due to size exclusion

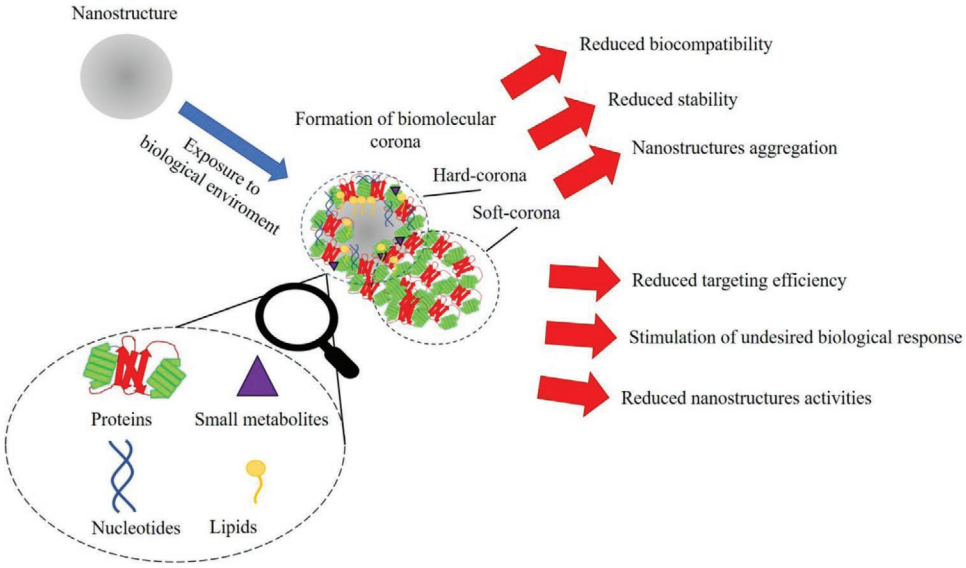

Figure 1. The composition of BC and its impact upon nanostructure properties.

related to pore diameter.[71] Nanostructures surface characteristics are another central parameter for determining the formation and characteristics of BCs. For example, the hydrophilicity and hydrophobicity of nanostructures play a major role in the formation and dynamics of BCs, and it has been shown that AuNPs with a hydrophobic surface can adsorb up to 2.1 times more proteins than hydrophilic particles.[21] The surface charge of nanostructures is one of the most important parameters in determining the formation and composition of BCs, but BC formation can cause significant changes to the surface charge of nanostructures, and can cause an inversion of charge polarity.[4,72–75] The presence of specific functional groups on the surface of nanostructures can also affect the formation of BCs. For example, amine groups of different types and densities has been shown to affect the BC formation process on AuNPs, along with how these particles interact with cells in vitro.[76] Surface nanostructures characteristics are the basis of BC formation, so it is not surprising that many surface functionalizations have been tested as a means to reduce or even prevent the association of undesired biological molecules with nanostructures. These anti-BC strategies are commonly referred to as "stealth" functionalization, and the most commonly used is the already mentioned coating of nanostructures with PEG.[77] However, PEG can only partially prevent the absorption of proteins and other biological molecules on the surface of nanostructures, but cannot completely prevent the formation of BCs. For example, it has been demonstrated that the FDA-approved Onivyde, a PEGylated liposomal drug, is able to form a BC when exposed to human plasma, and that this corona is extremely important in boosting the uptake of onivyde by the pancreas ductal adenocarcinoma cell line (PANC-1).[77] The efficiency of PEG coatings as a "stealth" functionalization has been linked to the molecular size of PEG used as a coating agent. For example, Natte et al. demonstrated that silica NPs coated with PEG at different MW form different PC when exposed to BSA, and that high MW PEG coatings are able to significantly suppress the formation of PC.[23] Other surface coatings and functionalizations that have been shown to affect BC-related processes include glucose and polyethylene glycol,[78] polyvinylpyrrolidone (PVP) and poly(2-vinyl pyridine)-*b*-poly(ethylene oxide) (PEO-*b*-P2VP),[79] zwitterionic moieties like cysteine,[27] a mixture of amine and zwitterionic moieties,[14] polyglycerol,[80] short-chain ethylene oxide (EO) oligomers,[81] poly(phosphoester)s,[82] and starch.[83] Another BC influencing parameter that can be associated with the administration of nanostructures, but that is not an intrinsic property of NPs themselves, is the presence of stabilizing surfactants. For example, the presence of cetyltrimethylammonium chloride together with polystyrene NPs has been shown to affect the composition of the BC formed on the surface of these nanostructures when exposed to plasma. In particular, the presence of cetyltrimethylammonium chloride caused the enrichment of apolipoprotein-A1 and vitronectin in the corona and a loss of clusterin, probably caused by the surfactant-induced denaturation of the protein.[84] The extrinsic parameter that mainly determines the characteristics of BCs is the molecular composition of the biological media to which nanostructures are exposed. For example, the relative concentration of proteins in biological media can affect the characteristics of BCs.[85] Fluid derived from different tissues (for example, the ocular environment) can cause the formation of dramatically different BC on the surface of nanostructures, thus determining the nanostructure–cell interactions.[86] The BC is also a species-specific phenomenon, as the exposure of nanostructures to biological media originating from different species can determine the associated BC that forms.[15,87,88] BC composition and characteristics can also vary greatly depending on whether nanostructures are exposed to in vitro or in vivo conditions, probably because in vitro experiments represent a far simpler environment than that of living organisms.[89–91] One main difference between in vitro and in vivo environments is the lack of flow and dynamic conditions. The exposure of nanostructures to static or dynamic biological media can cause dramatic differences in BC composition, due to the effect of flow-applied shear stress, and these BC differences can even affect the biological activities of nanostructures.[25,61,92,93] The exposure of nanostructures to the biological media derived from disease-affected subjects can lead to the formation of a BC that is very different from that obtained after exposure to biological fluids derived from a healthy subject.[94] As we discuss in the next paragraph, this patient-derived BC is usually composed of disease-specific biomarkers that can be used as a diagnostic tool. Although the phenomenon of BC is commonly associated with the exposure of nanostructures to animal-derived proteins, it has been demonstrated that exposure to plant-derived proteins and molecules can also cause BC formation, as can be intuitively expected. This could have potentially disruptive implications for environmental studies, due to the inevitable exposure of plants to industrially derived nanostructures. Prakash and Deswal investigated the formation of plant-derived BCs in detail, and exposed AuNPs to *Brassica juncea* leaf crude protein and a nuclear-enriched fraction.[95] As previously mentioned, BC–nanostructure complexes are not static systems but can undergo significant change in terms of composition and structure, due to external stimuli. For example, BCs can evolve over time when exposed to different biological sources, as demonstrated by Lundqvist et al., who found that when moved from plasma to cytosolic fluid, both silica and polystyrene NPs change their BC composition, although a "fingerprint" of the original corona was still present.[96] BCs can be affected and changed by enzyme activity, and the rate of degradation is affected by the protein composition of the corona itself.[97] Temperature can affect both the composition of BCs and the molecular structure of the moieties associated with nanostructures surface. Mahmoudi et al. showed that small temperature changes can affect the composition of the BCs formed on the surface of superparamagnetic NPs (SPIONs) and can also change the response of cells exposed to particles with BC formed at different temperature.[98] Using a similar approach, magnetic iron oxide NPs exposed to calf serum was demonstrated to result in an increase in the level of protein attached to their surface, depending on the exposure time, and this effect was less significant when the particles were exposed to the proteins at a temperature above 50 °C.[99] Temperature changes induced by the nanostructures themselves can also affect the BC composition, as in the case of plasmonic heating (a process typical of some nanostructures, in which heat is generated through irradiation with light at a specific wavelength), which has been shown to affect the

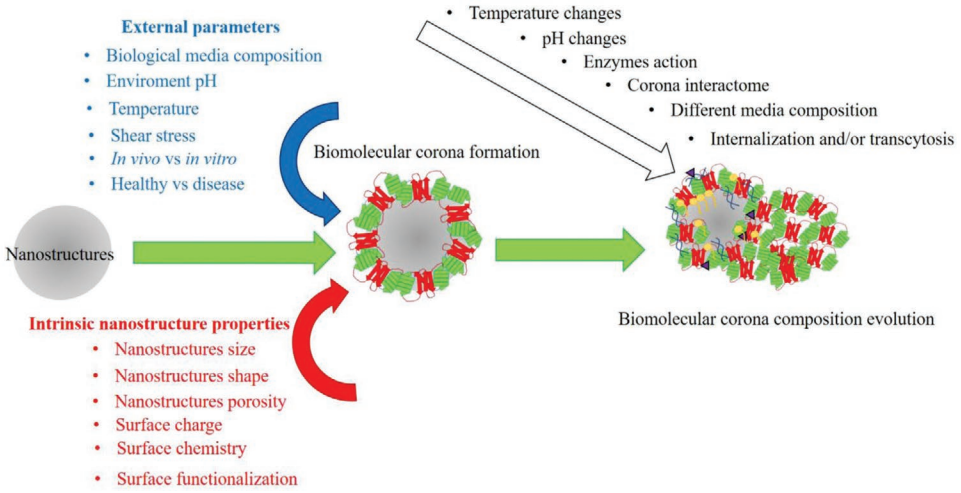

Figure 2. Schematic representation of the parameters affecting the formation, composition, and evolution of BC associated with nanostructures after exposure to a biological environment.

composition of BCs associated with gold nanorods.[100] The association of molecules with nanostructures surface, in particular proteins, can also affect the thermal stability of the molecules themselves. For example, the formation of particle–BC complexes can significantly change the temperature stability of proteins like transferrin, with a change in the unfolding temperature of up to 10 °C.[101] The presence of unfolded or heat-inactivated protein in the BC is extremely important in determining the interactions of nanostructures with biological systems. Heat-inactivated protein associated with BC can affect the biological functionality and cellular interaction of nanostructures. Unfolded protein on the surface of the nanostructure can induce the association of an unfolded protein response (UPR) and heat shock proteins with nanostructures can induce potentially adverse effects in cells.[102] Finally, BCs can evolve after exposure to a biological environment through subsequent interactions with different tissues and cellular population, as in the case of crossing the blood–brain barrier (BBB)[103] or other forms of cellular transcytosis-mediated transporting of BC–nanostructure complexes.[104] A schematic representation of the parameters affecting the formation, composition and evolution of BC is provided in **Figure 2**.

2.3. Opportunities for Biomolecular Corona Exploitation

Our review demonstrates that BC formation and composition is complex and is affected by a large variety of parameters and can lead to unexpected and undesired alterations of nanostructure functionality. However, the formation of BCs under controlled conditions has also been exploited as a new and exciting tool that can improve nanostructure properties and even lead to new functionality in nanodevices. One of the most common uses of BCs is in diagnosis. For example, it was shown that positively charged AuNPs exposed to ovarian cancer cell lysate were able to form a BC enriched with hepatoma-derived growth factor (HDGF). This has been proposed as a potential tool for ovarian cancer diagnosis.[105] Lipid nanostructures exposed to the blood of pancreatic cancer patients showed an increase in protein content associated with their surfaces when compared to particles exposed to the blood of healthy subjects.[106] In a similar study, AmBisome-like liposomes exposed to the plasma of pancreatic cancer patients were found to evolve a BC that was significantly different, both in terms of charge and composition, to that derived from exposure to the plasma of both healthy subjects and subjects affected by other forms of cancer.[107] Similar results have been obtained with other classes of nanostructures exposed to the serum of patient affected with triple-negative breast cancer. Here, the BC associated with the surface of the nanostructures after exposure to the serum of the cancer patients was enriched by breast cancer-specific molecular markers.[13] The diagnostic potential of nanostructure-associated BC is not limited to cancer. For example, the exposure of silica nanostructures to the lung fluid derived from either healthy or asthmatic patients resulted in the formation of different BCs.[108] The diagnosis exploitation of nanostructures associated with BC is not limited to its protein components. For example, it has been shown that 10 nm core sized magnetic NPs with carboxylic acid coating were able to capture microRNA on their surface after exposure to urine samples, and that these miRNA can be used as potential biomarkers.[3] The diagnostic potential of BCs is not limited to human healthcare. For example, the BC formed on the surface of surface active maghemite NPs (SAMNs) after exposure to bovine whey has been used to isolate specific biomarkers of cow mastitis.[109] The BC has also commonly been used as a means of improving nanostructure biocompatibility. For example, the formation of BCs on the surface of metallic nanostructures after exposure to serum was able to reduce the oxidative stress caused by these nanostructures when interacting with cells.[7] Similar results were obtained for the phototoxicity associated with TiO_2 nanostructures, which can generate reactive oxygen species (ROS) after UV irradiation. The preincubation of TiO_2 nanostructures with serum has been shown to modulate this ROS-generating ability, due to the free radical trapping properties of the nanostructure-associated BC.[110] This improvement in BC-mediated nanostructure biocompatibility can be caused by both hard and soft

corona, as is the case for silver nanostructures. Silver composites are known to release silver ions and that these are involved in silver nanostructures toxicity. However, BC has been shown to reduce this effect, with the hard corona acting as a sulfidation site and the soft corona trapping silver ions as silver sulfide nanocrystals, resulting in a reduction of silver nanostructures toxicity.[111] The formation of BCs has been also demonstrated to reduce the cytotoxicity of graphene oxide,[112] Au@Fe_3O_4 Janus particles,[18] and carbon quantum dots.[113] BC has also been used to improve the hemocompatibility of nanostructures, such as for amorphous silica NPs with diameters of 70 nm (nSP70) and NH_2 surface modification, where the exposure to serum protein led to higher binding of the coagulation factor XII. This higher binding to NH_2 rich particles caused a reduction in the abnormal activation of the coagulation cascade, as reported for nSP70 without NH_2 surface functionalization.[114] Although BC can harm nanostructure targeting properties, several works in the literature describe the opposite, demonstrating that the exploitation of BCs can specifically target nanostructures or reduce the interaction of nanostructures with off/targets. For example, Chen et al. designed specific lipid nanostructures by manipulating their lipid composition, thus producing nanostructures able to recruit apolipoprotein in their corona, which increases their cancer-targeting efficiency.[115] The precoating of nanostructures with apolipoprotein E4 has been also proposed as a means of overcoming the BBB, and thus potentially enabling the delivery of nanostructures to the brain.[116] In nanostructure-mediated targeting, another example of BC, retinol-conjugated polyetherimide (RcP) NPs were developed and designed to recruit specifically retinol-binding protein 4 in their corona, thus enhancing their ability to target hepatic stellate cells.[20] In a more complex functionalization procedure, the precoating of nanostructures with a fusion protein composed of a HER2-binding affibody with glutathione-S-transferase was used as a strategy to hinder the formation of BCs on exposure to biological media, while retaining targeting efficiency.[8] The BC has also been used as a tool for the isolation of circulating tumor cells (CTCs). Fe_3O_4 NPs covered by a serum-derived BC interacted with CTCs from blood samples derived from colorectal cancer patients. This enables the separation of CTCs from other blood cells.[117] The BC has also been used to modulate or reduce the interaction of nanostructures with immune cells.[26] For example, the association of black phosphorus nanosheets with BCs can modulate the polarization of macrophages on exposure to these nanostructures,[118] and the precoating of polystyrene nanostructure with immunoglobulin depleted plasma resulted in lower particle uptake levels by immune cells.[119] The preformation of BCs on the surface of particles has also been shown to be a viable strategy for increasing the bioavailability of nanostructures. For example, the precoating of liposomes with human plasma protein was found to drastically reduce the capture of these nanostructures by circulating leukocytes, thus increasing their circulation.[120] BCs can also be used more actively, for example, as a means of achieving the loading of nanostructures with active moieties. The BC formed after the exposure of silica NPs to serum-containing media was used to load these particles with doxorubicin and meloxicam, and the functionalized NPs showed a strong antiproliferative effect against osteosarcoma cells.[121] Similarly, the BC formed after the exposure of bimetallic gold nanorods to albumin and transferrin was used to functionalize nanostructures with doxorubicin.[122] Other examples include the use of BCs to functionalize gold nanorods with the photosensitizer Chlorin e6 (Ce6) as a tool for in vivo photodynamic and photothermal therapy,[123] and the use of BCs as a means to functionalize AuNPs with DNA.[124] The BC has also shown great promise in vaccination. For example, AuNPs exposed to avian coronavirus spike proteins have shown the ability to form a particle–BC structure resembling the natural viral particles. These particle–PC complexes were also more efficient as a vaccination agent compared to inoculation with only free protein.[125] Zhang et al. also presented an interesting use of BCs. They engineered nanozymes to generate either "hard" or "soft" BCs on their surface. The formation of the BCs (in particular the hard type) led to an inhibition of nanozyme activity. However, when the nanozyme is internalized by cells, the endogenous protease of the cells reactivated the nanozymes by removing their associated BC.[126] Zeng et al. also found that treating a cancer patient with cisplatin led to the formation of platinum NPs covered by a BC, due to the interaction between platinum and blood proteins. These platinum NPs have been found to accumulate in tumors, thus inhibiting their growth and leading to cancer cell death.[127] In another application, bovine beta-lactoglobulin (β-LG) associated with AuNPs were used as a biocompatible stabilizing agent to develop nanoplatforms able to act as both *Escherichia coli* biosensing devices and an edible form of computed tomography (CT) contrast agent for gastrointestinal tract imaging.[128] BC has also been applied in molecular tests and assays. For example the BC formed on the surface of insufficient polyhedral oligomeric silsesquioxane (POSS) polymer-caged AuNPs (denoted as PP–AuNPs) was used to determine the concentration of metallothioneins through a colorimetric reaction.[129] In another approach involving BCs in a molecular biology protocol, Chan et al. utilized DNA functionalized AuNPs able to hybridize to the mRNA 3′-untranslated region of insulin and green fluorescent protein (GFP). Once exposed to the cell lysate of Hela cells, these DNA–AuNPs were able to recruit a BC composed of both ribosome and translation factors, and to enable the translation and production of both insulin and GFP in higher quantities than bare mRNA sequences.[130] Finally, BCs have been applied in antidote development. O'Brien et al. fabricated and optimized polymeric NPs for the recognition and the sequestration of venomous PLA2 enzymes present in the bloodstream.[131] Examples of applications of the BC phenomenon are listed in **Figure 3**.

3. Techniques Used for Biomolecular Corona Analysis

As previously mentioned, many techniques have been used to characterize the BCs formed on nanostructures when interacting with biological fluids. These range from relatively simple spectroscopy techniques to more complex tests involving high throughput analysis like mass spectroscopy or direct imaging approaches. In this section, we provide a complete overview of

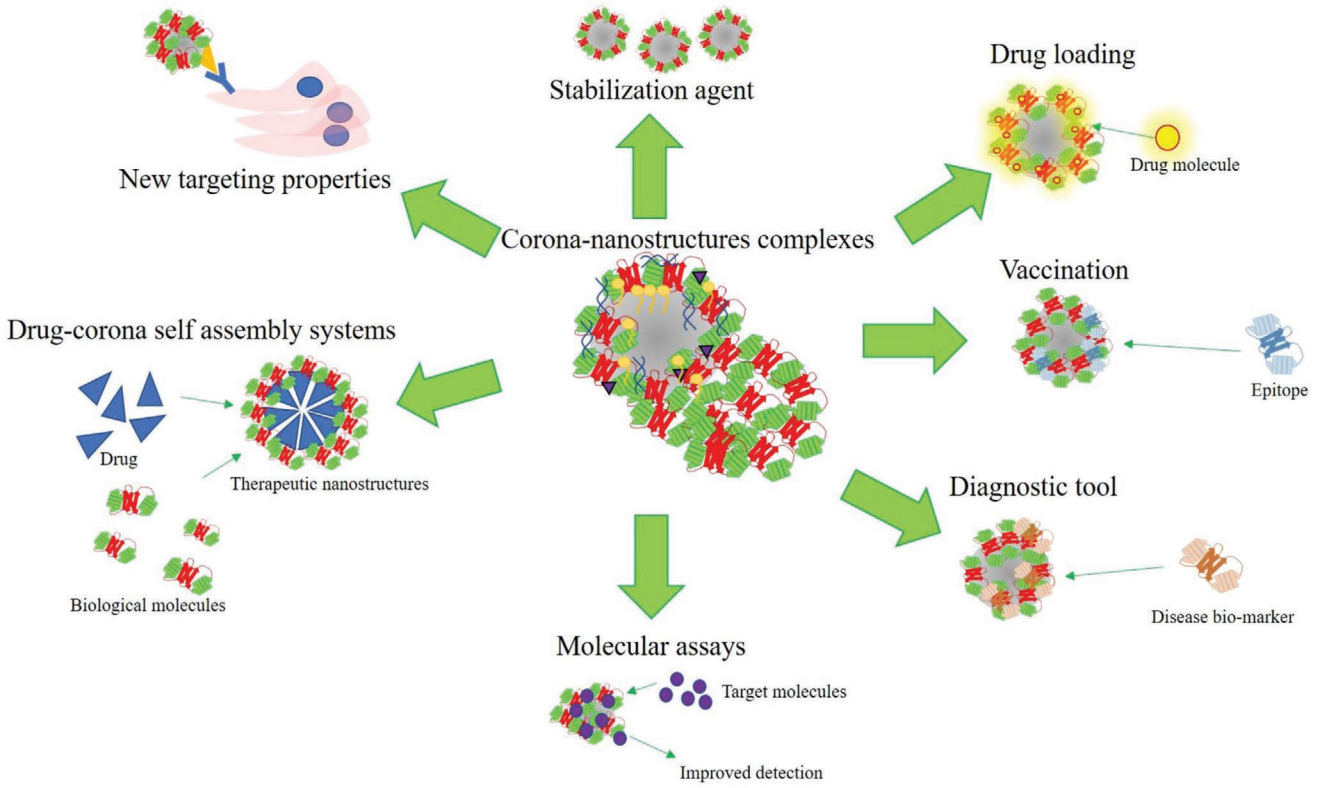

Figure 3. Examples of exploitation of the BC phenomenon in biomedical applications.

all the techniques currently used in the characterization of BCs, analyzing the level of information they provide and comparing the advantages and drawbacks of each approach. The techniques are be distinguished into four types:

1) Bulk material techniques, based on indirect scattering, spectroscopic, and fluorescence measurements;
2) Colorimetric and enzymatic assays;
3) High throughput techniques, based on gel electrophoresis and/or proteomic analysis such as mass spectroscopy;
4) Direct imaging techniques, based on various forms of microscopy.

Various other techniques are based on several different approaches, which are not common but can still provide interesting information about BC characteristics and composition.

In this section we discuss the currently available techniques for analyzing BCs, to give the reader an overview of current BC studies and to contextualize the role that RAMAN microscopy can play in BC analyses in the near future.

3.1. Indirect Techniques Based on Scattering, Spectroscopy, Colorimetric Analyses, and on Fluorescence Indirect Measurements

One basic type of analysis for assessing the presence of BCs is obtaining hydrodynamic diameter measurements through DLS analysis. Commonly plain nanostructures and nanostructures exposed to biological fluids are compared based on the DLS measurements.[9] Exposure to biological fluids typically leads to an increase in the hydrodynamic diameter caused by the formation of a BC on the surface of the NPs. DLS analyses are usually combined with zeta potential measurements to assess the surface potential of nanostructures. Similar to DLS analyses, the exposure of nanostructures to biological fluid commonly leads to changes in the surface charge of the nanostructures themselves, caused by the bonding of protein and other biological molecules on the surface of the nanostructures.[9,23,101] Both DLS and zeta potential analyses are extremely fast assays that can be performed with relative ease on a wide variety of nanostructures, thus providing information about the effect that BCs have on the nanostructures' hydrodynamic diameters, surface charge, and overall stability. However, the BC information derived from these analyses is relatively limited, providing little to no data about BC quantity, shape, or composition. An extremely fast and easy way to quantify components of the BC is through colorimetric assays. The total amount of proteins associated with nanostructures is commonly assessed through colorimetric assays like the Bradford assay, Pierce 660 assays, or BCA tests.[11,87,122] The basic principle of these tests involves the binding of specific dyes to proteins, resulting in a shift in the absorption spectra of the dye molecules, which is directly related to the concentration of protein molecules.[11,87,122] The presence of specific proteins can be assessed through the use of enzymatic activity assays, which identify active enzyme molecules associated with nanostructures.[95] The main advantages of enzymatic activity assays are that they can confirm the

presence of specific molecules associated with nanostructures and can also assess their functionality.[95] As previously noted, BCs are not only composed of proteins, so assays for the detection of lipids like cholesterol and triglycerides have been used to analyze BC composition.[1,63] Spectroscopy has also shown potential in the analysis of BC formation, and in several cases, the binding of molecules on the surface of nanostructures has been shown to change their absorption spectra. For example, for graphene oxide, silver nanostructures, gold nanostructures, and gold/silver nanoalloy, the incubation with proteins can change the peak of absorption corresponding to their surface plasmon resonance (SPR) wavelength, both in terms of intensity and wavelength.[5,28,79,132] As Dominguez-Medina et al. note in their analysis of protein adsorption and subsequent unfolding on the surface of gold nanorods, the effect observed with the formation of BCs on nanostructures UV–vis absorption spectra may also be caused by an increase in the nanostructures aggregation levels.[5] UV–vis spectra analysis can also be used to analyze the effect of the formation of BCs on the structure of the proteins associated with the nanostructure, such as in the study by Yang et al., where the structural changes induced on bovine hemoglobin (BHb) upon exposure to hydrophilic and hydrophobic silica NPs were analyzed through UV–vis spectroscopy.[22] Fluorescence spectroscopy is also commonly used to analyze BC and nanostructure–protein interactions. For example, the endogenous fluorescence of proteins can be used to track their binding to nanostructures.[16,49] A common fluorescence-based approach in the study of BC involves the use of fluorescence quenching phenomena, which is the reduction of fluorescence intensity caused by the proximity of fluorophores with nanostructures. In some studies, fluorescence quenching of both the endogenous fluorescence of proteins and fluorescently labeled proteins has been used to investigate the interaction between proteins and nanostructures.[24,40,133] One interesting example of fluorescently labeled protein use in BC studies is the work by Pinals et al., in which the exchange rate of two fluorescently labeled blood abundant proteins (namely, fibrinogen and albumin) on the surface of single-walled carbon nanotubes (SWCNTs) were investigated, functionalized with single-strand DNA (SSDNA) acting as a biosensor for dopamine.[133] The binding of both proteins and SSDNA fluorescently labeled on the surface of the SWCNT was monitored through the fluorescence quenching effect caused by the proximity of the fluorophore to the SWCNT surface. In addition, the binding of protein to the surface of SWCNT can attenuate the sensor response to dopamine. Fibrinogen showed a higher affinity for the SWCNT and a greater effect on sensor efficiency. These studies provide interesting data both in terms of binding kinetics and the BC effect on nanosensor activity.[133] Although fluorescence spectroscopy has interesting applications in BC studies, fluorescently labeled proteins are more commonly used in microscopy-based approaches, which are discussed in detail later in this paper. Finally, FTIR has also been used as a technique to investigate BC phenomena. Some examples include the characterization of BCs associated with silver/gold nanoalloy,[28] the characterization of proteins associated with iron oxide magnetic NPs and SPIONs,[16,24] and the analysis of the interaction between BHb and silica NPs,[22] of blood-derived BCs on the surface of 2D model nanosheet structures of molybdenum disulfide (MoS_2),[6] of protein association on the surface of gold nanostructures with different shapes, and of PC formation on the surface of polyacrylic acid-coated cobalt ferrite NPs (PAA NPs) and silica NPs.[134]

3.2. Gel-Electrophoresis and Mass Spectrometry

Gel electrophoresis-based approaches and MS proteomic analysis represent the most widely used techniques to obtain information about the composition of BCs associated with nanostructures.[10–21] The protein composition of BCs is commonly analyzed by gel-electrophoresis performed in denaturing conditions (usually through the use of SDS-PAGE gels). The combination of the gels with protein-specific labeling techniques (for example coomassie blue staining procedures) is an easy, rapid, and relatively cheap method of obtaining information about the relative molecular weight of proteins associated with nanostructures.[135] To assess the presence of specific proteins, western blot analyses can be performed using specific antibodies directed against the proteins.[135] Other forms of gel-electrophoresis have been used, although less frequently, to provide information about BC compositions. 2D-page assays involving the migration of proteins through two orthogonal dimensions (a pH gradient and an electric field) are able to separate proteins based on both isoelectric point and dimensions. This is typically a necessary step in analyzing complex protein mixtures and has been used in BC studies.[136] Native PAGE, or gel electrophoresis performed in nondenaturing conditions, has also been used (although less frequently than SDS-PAGE) to examine the proteins associated with nanostructures in their native conformation.[10] The gel separation of proteins is typically the first step for purification before a proteomic MS analysis. MS is, without doubt, one of the most powerful, extensive, and necessary tool in BC studies. The basic principle of MS involves the ionization of the sample's molecules, the subsequent separation of obtained ions according to their mass-to-charge ratio, and the detection of charged particles through a detection mechanism (e.g., an electron multiplier).[137] The results are typically presented as a plot spectrum relating intensity to mass-to-charge ratio. MS is therefore able to identify an enormous number of molecules, enabling the characterization of the molecular composition of nanostructures associated with BCs. MS is also able to identify (directly or indirectly) nonproteic molecules associated with nanostructures, like lipids or polysaccharides, leading to a complete understanding of the BC molecular composition.[2,63] Thus, MS is a necessary analytical method in BC studies and should be included in any investigations involving the interaction of nanostructures with complex biological fluids. However, MS alone cannot give a complete understanding of BCs, first because it cannot provide information about the BC associated with single nanostructures or about BC heterogeneity within the same sample of nanostructures. In addition, MS cannot be used to study parameters like BC kinetic formations over a short time scale, the shape and distribution of molecules on the surface of nanostructures, or the dynamic evolution of BC composition. Therefore, MS should always be combined in BC studies with other techniques like microscopy analyses, to enable a full understanding

of the dynamic interactions between nanostructures and biological molecules.

3.3. Microscopy-Based Approaches

The main advantage of microscopy-based approaches in the study of BC is their ability to analyze an extremely small quantity of nanomaterials, up to single nanoparticles and even single molecules of proteins. Due to the high spatial resolution of microscopy techniques, it is possible to investigate BC characteristics and properties that would otherwise be impossible to assess. with other techniques, for example, heterogeneity in BC composition within the same sample of nanostructures can be assessed, investigate in real-time dynamics of BC evolution on a small subset of nanostructures investigated, and BC shape and morphology at the level of single nanostructures can be examined. Fluorescence microscopy is commonly used to combine fluorescently labeled proteins with either autofluorescent or fluorescently labeled nanostructures to investigate their interactions. In BC studies, confocal microscopy is more common than an epifluorescence setup, due to the higher spatial resolution obtained through the confocal apparatus. Studies involving confocal microscopy in BC investigations include examining how BCs form on the surface of various nanostructures evolve after cellular uptake[138] and the characterization in situ of the formation and temporal evolution of BCs on the surface of silica NPs in an underflow condition.[139] One of the major drawback of epifluorescence and confocal microscopy is their relatively low spatial resolution when compared to other microscopy techniques, which limits their ability to image single nanostructures that are small in size. Lin et al. proposed an approach based on the combination of ultrafast dark field microscopy with an analysis of rotational diffusivity, to examine the BC associated with a single nanostructure in situ. Lin et al. were able to use a rotational diffusion coefficient analysis to measure the size increase caused by the binding of protein molecules onto the surface of gold nanorods.[140] Super-resolution microscopy has also been proposed in BC studies to address the limitations posed by optical microscopy approaches. Stochastic optical reconstruction microscopy (STORM) has been applied to the study of BCs at the level of single nanostructures and single protein molecules. The most interesting STORM application in BC studies is in the study of Feiner-Gracia et al., in which STORM microscopy was used to analyze and quantify the number of protein molecules associated with mesoporous silica NPs. Feiner-Gracia et al. were able to demonstrate not only the presence of high heterogeneity in terms of protein adsorption on the surface of silica NPs, but also how this is affected by both the exposure time of nanostructures to the protein source and by the surface chemistry of the NPs themselves.[141] In another example, the TiO_2 nanostructure interaction with protein and the temporal evolution of BCs associated with TiO_2 nanostructures (with different surface functionalization) after cellular uptake was examined using STORM microscopy analyses.[142] Finally, examining luminescence correlation decays through confocal microscopy analysis has been also proposed as a method of investigating the interaction between BSA and cationic mercapto-undecyl trimethylammonium bromide coated gold nanorods.[5] Electron microscopy, in particular SEM and TEM, are also invaluable tools for the analysis of nanostructures associated with BCs, due to their higher spatial resolution when compared to optical techniques. Although some applications have been demonstrated,[24–27] SEM is far less common than TEM in BC studies, probably due to the technical difficulty of providing a clear image of both nanostructures and the associated BC. The more commonly used TEM has been extensively applied, for example through the analysis of PC formation on the surface of both plain and PEG functionalized silica NPs,[23] the imaging of silver/gold nanoalloy exposed to HSA,[28] the imaging of the in vitro and in vivo PC associated with liposomes,[89] cryo-TEM imaging of silica and poly(vinyl) acetate (PVAc) associated BC corona after exposure to respiratory tract lining fluid (RTLF),[94] imaging of the PC formed on the surface of magnetic iron oxide NPs (MIONPs),[24] imaging of intestinal fluid-derived PC formed on the surface of ascorbyl-palmitate derivatives' nanoemulsion,[143] and the analysis of platinum NPs associated with BC formed in the bloodstream of patients after cisplatin treatment.[127] Electron microscopy can also be combined with energy dispersive X-ray spectrometry (EDS) analysis to investigate the elements present in nanostructure–BC complexes.[127] An interesting example of the application of electron microscopy in BC studies is the work of Kokkinopoulou et al. TEM imaging is here combined with proteomic analysis and a differential centrifugation procedure for nanostructures purification, and Kokkinopoulou et al. were able to provide direct images of both the soft and hard corona formed on the surface of silica NPs, showing that PC appears like an undefined network of protein enveloping the nanostructures.[144] TEM has also been successfully applied to map the epitopes of ApoB-100 present on the surface of silica NPs after exposure to serum proteins, not only providing information on the position of the functional epitope after exposure to biological fluids but also demonstrating that nanostructures can acquire a biological motif due to BCs, which can lead to undesired side interactions of the nanostructures themselves with biological systems.[145] In a recent application, cryo-TEM combined with cryo-electron tomography and computational simulation has been used to tridimensionally map at a nanoscale resolution the interaction, association, and distribution of biomolecules on the surface of single nanostructures.[146] Finally, AFM has proven to be a useful tool for imaging BC associated with nanostructures and their mechanical properties. For example, AFM has been used to investigate the association of protein molecules with silica NPs functionalized with polymers at different molecular weights.[23] In another example, AFM was used to demonstrate how the interaction between dihydrolipoic acid (DHLA) protected gold nanoclusters (DHLA-AuNCs) with proteins (transferrin and human serum albumin) caused the formation of protein aggregates.[147] Other examples include the analysis of the morphology and size of polymeric nanostructures (poly(lactic-*co*-glycolic acid) (PLGA), 1,2-distearoyl-*sn*-glycero-3-phosphoethanolamine-poly(ethylene glycol) (DSPE-PEG), polystyrene nanostructures functionalized with various surface chemistry and loaded with a hydrophobic fluorogen with aggregation-induced emission characteristic) associated with various proteins,[148] the characterization of graphene oxide associated with serum proteins;[112] the characterization of the PC formed

on the surface of poly(methyl acrylate) (PMA) nanocapsules;[149] imaging of the PC associated with magnetic mesoporous silica nanostructures;[67] and both the imaging and young modulus analysis of the PC associated with liposomes and leukocytes after in vivo exposure.[150]

3.4. Other Techniques

In this paragraph, we analyze the techniques used in BC nanostructure interaction analysis that are either aimed at investigating very specific aspects of the BC phenomenon (like protein secondary structures or thermodynamic properties) or that are interesting but limited in their application. One open question in BC studies involves the conformational state of the molecules (in particular proteins) associated with nanostructures. CD has been applied to this issue by investigating the structure of proteins involved in BCs. CD can be applied to measure the secondary conformation of proteins, and in particular the ellipticity values at 208 and 222 nm can be used to estimate the α-helical content of proteins involved in BC formation.[28] This approach has been used for evaluating the presence of soft or hard corona on the surface of polystyrene nanostructures, on the conceptual basis that proteins involved in soft corona should be able to maintain their secondary structure organization more easily than proteins involved in hard corona.[4] Other applications of CD in BC studies are generally aimed at understanding the conformational changes generated by the interaction of proteins with various nanostructures.[4,5,28,132,151] CD has also been used to study the thermal stability of proteins associated with SPIONs.[101] Thermal-based analyses have been used to understand and characterize the phenomenon of BCs. The two main thermal-based techniques are thermal gravimetric analysis (TGA) and isothermal titration calorimetry (ITC). TGA is based on the measurement of a sample mass during controlled temperature changes. TGA has been used in BC studies as a means of determining the mass of proteins associated with nanostructures.[71,99] ITC is used to study the thermodynamic parameters of interaction (such as stoichiometry, enthalpy, or binding affinity) of molecules in solution. ITC has also been used to investigate the thermodynamic parameters involved in the interaction between protein and polystyrene NPs functionalized with various poly(-phosphoester)s (PPEs);[82] to understand the thermodynamics of protein association with silica NPs and how these parameters are affected by the solution condition and NPs surface chemistry;[152] to demonstrate the exothermic nature of BSA binding to silver nanocolloids;[79] to determine the "preference" of protein binding to either cationic or anionic nanostructures;[45] to discriminate between "primary" and secondary protein binders on the surface of gold nanostructures;[153] and to characterize the binding thermodynamics of nonprotein molecules on the surface of polystyrene nanostructures, in particular lipids associated with lipoproteins.[63] Another technique based on thermal analyses used in BC studies is the microscale thermophoresis (MST). MST is based on the measurement of the changes induced by temperature on the fluorescence of the molecule/structure of interest. Fluorescence changes are related to two distinct phenomena: the effects of temperature-related intensity changes (TRIC), which describes the property of changing fluorescence intensity in fluorescent objects due to temperature, and thermophoresis, which describes the movement of the molecules/structure of interest along temperature gradients. MST is commonly used to determine the binding affinity of biomolecules and has been applied to studying the interaction of nanostructures and biomolecules. MST has been applied in the analysis of poly(ethylene glycol)-*block*-poly(D,L-lactide) (PEG-*b*-PLA) interaction with proteins as a method of relating the affinity of protein particles to in vivo outcomes;[154] in investigating how the morphology of gold nanostructures can affect their affinity for proteins;[70] and to determine the binding affinity of different proteins to silica nanostructures.[155] Carril et al. proposed a new approach based on ^{19}F diffusion nuclear magnetic resonance (NMR) spectroscopy. They measured the hydrodynamic radii of different nanostructures exposed to complex media (either blood or plasma) marked with ^{19}F, using NMR diffusion spectroscopy, which can characterize in situ the evolution of nanostructures size due to exposure to biomolecules.[156] Small-angle scattering (SAS) techniques like small-angle X-ray scattering (SAXS) and small-angle neutron scattering (SANS) have also been used to characterize BC associated with nanostructures. In SAXS, the sample is irradiated with a monochromatic beam of X-rays that can a) pass the sample without interacting with it, or b) be scattered. The scattered X-rays can be collected and analyzed to provide information about the structure of the sample itself. Small-angle neutron scattering is very similar in principle, but the sample is irradiated with a neutron source instead of an X-ray beam, and neutrons are scattered by either nuclei interaction or interaction with impaired electrons. SAXS has been applied to study how BC affects the lipid layer properties of PEGylated CLs[55] and how BC formation affects the inner lipid structure of lipoplexes.[157] SANS has been used to characterize the interaction between polystyrene NPs and HSA in terms of soft corona and hard corona geometry and interparticle interaction,[4] and also to investigate the thickness, geometrical organization, and molecular structure of PC formed on the surface of silica NPs.[158] Although not directly related to the analysis of BCs, Di Silvio et al. examined their effect by taking an interesting approach based on neutron reflectometry. They investigated how the presence of BCs changed the interaction between NPs and the lipid membrane. By combining NR with a quartz microbalance with dissipation monitoring (QCM/D), they were able to analyze the effect on the structure of a supported lipid bilayer (SLB) of the presence of PC on the surface of polystyrene NPs upon interaction, demonstrating that the soft corona can permanently alter the lipid bilayer organization.[159] X-rays have also been applied, through X-ray absorption spectroscopy and X-ray microbeam fluorescence analysis, to investigate the binding of BSA to gold nanorods, with particular consideration of the characterization of the protein–nanostructure binding site.[160] Differential centrifugal sedimentation (DCS) is a technique that has gain attention in recent years, and is based on the analysis of the sedimentation time of NPs through a fluid when exposed to a centrifugal field.[161] This sedimentation time is related to both particles size and density. The technique has been successfully used to characterize the change in size and density caused by the formation of BCs associated with SPIONs, silica, and

polystyrene nanostructures.[90,98,145,155,162] Field-flow fractionation (FFF) has been proposed as a tool to separate nanostructures based on their associated BC. Both symmetrical and asymmetrical FFF have been applied to study the BCs of poly(organosiloxane) NPs, SPIONs, and polystyrene nanostructures.[163–165] Finally, it should be noted that the intrinsic characteristics of certain groups of nanostructures can be used to investigate the BC formation phenomena. The most representative example is probably magnetic nanostructures, which due to their interaction with various forms of external magnetic stimulation represent an optimal benchmark for the characterization BC. First, the magnetic properties of magnetic nanostructures have been used as a tool to separate and purify them in complex media by attracting them with a static magnetic field.[99] Specific analysis methods such as magnetorelaxometry (MRX) and hysteresis curves analysis have been used to compare the magnetic properties of SPIONs and BC coated SPIONs, providing informative data about BC quantity and its effect on nanostructure aggregation.[99]

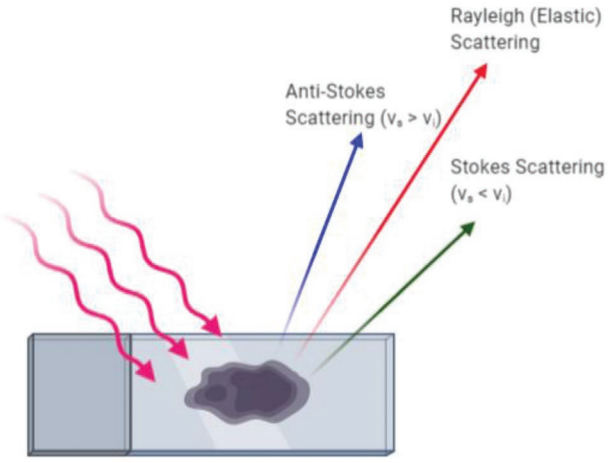

Figure 4. Elastic and inelastic scattering of light as a result of its interaction with matter.

4. Raman Spectroscopy and Biomolecular Corona Studies

4.1. Theory of Raman Spectroscopy

Raman spectroscopy is based on the molecular vibrations of compounds and is very useful in terms of material characterization. Information about molecular vibrations can be obtained by using the interaction of light with the sample. When an incident light interacts with the electron cloud of molecules, it polarizes the electron cloud and excites the electrons into a virtual state. Excited electrons are not stable, and they must relax by scattering photons in all directions. The scattered photons generally have the same frequency and wavelength as the incident light and this type of elastic scattering is known as Rayleigh scattering. Raman and Krishnan identified inelastic scattering as a new type of secondary radiation in 1928.[166] After the interaction of light with the sample, the scattered photons can be collected and the frequency and the intensity of those that are scattered inelastically can be used to construct a Raman spectrum. Raman spectroscopy is based on the effects of force constants and bond distances of atoms; these cause a shift in the wavelength of scattered light. This shift in the wavelength occurs due to energy conservation. If the energy of the incident photon is much greater than that of the scattered photon, Stokes Raman scattering takes place, which is observed as a red shift in the spectrum. If the photons gain energy due to their interaction with matter, anti-Stokes Raman scattering takes place, and the wavelength of the incident photon is blue-shifted. The polarizability of electron clouds and the overall properties of vibrations affect vibrational intensities, which leads to the formation of characteristic "fingerprint bands" of a molecule. These bands occur at different wavenumbers specific to the type of vibrational modes and the changes in the frequency of radiation, due to the interaction of molecular vibrations. They can be detected by using Raman spectroscopy, and this phenomenon makes the detection and identification of molecules much easier.[29,167] A representation of Rayleigh and Raman scattering is shown in **Figure 4**.

Techniques based on Raman spectroscopy have many advantages, particularly if the research aim is to analyze biological samples such as proteins, lipids, or even cells. There is no need for sample preparation or the labeling of molecules before analysis. In addition, water molecules in the sample do not affect the Raman spectrum, making it possible to analyze the samples in solution without any drying process.[168] Another advantage of Raman spectroscopy is its high selectivity, meaning that the shifts in wavenumbers are specific to the molecules. If a molecule such as a lipid, amino acid, or nucleic acid is present in the sample, specific peaks related to the chemical structure of the molecule can be observed in the spectrum.[169]

Although Raman spectroscopy has many benefits, it also has some limitations. The main limitation is the low occurrence of Raman scattering. Naturally, most of the light scatters elastically, and only a small proportion scatters inelastically.[170]

To overcome this limitation, methods of increasing the sensitivity and intensity of Raman signals have been developed. The enhancement of Raman scattering in the presence of a metallic substrate was first observed by Fleischmann et al.[171] This was an unintended discovery, as the main aim of the study was to use Raman spectroscopy to distinguish two types of pyridine adsorption on the surface of a silver electrode. An increase in signal intensity of 10^6 times was observed in this experiment, which led to the development of SERS. This innovation made it possible to work with analytes in low concentrations and has since become a useful tool for the detection of small molecules and drugs.[172,173]

4.2. Surface-Enhanced Raman Spectroscopy

As mentioned above, in a light scattering process, the number of inelastically scattered photons is very low, which makes it difficult to detect the Raman signals. The parameters of laser power and acquisition time can be sustained at a high level to increase the signal intensity. However, exposure to high laser power for a long time may cause the sample to decompose, particularly if it is composed of biological molecules or cells.

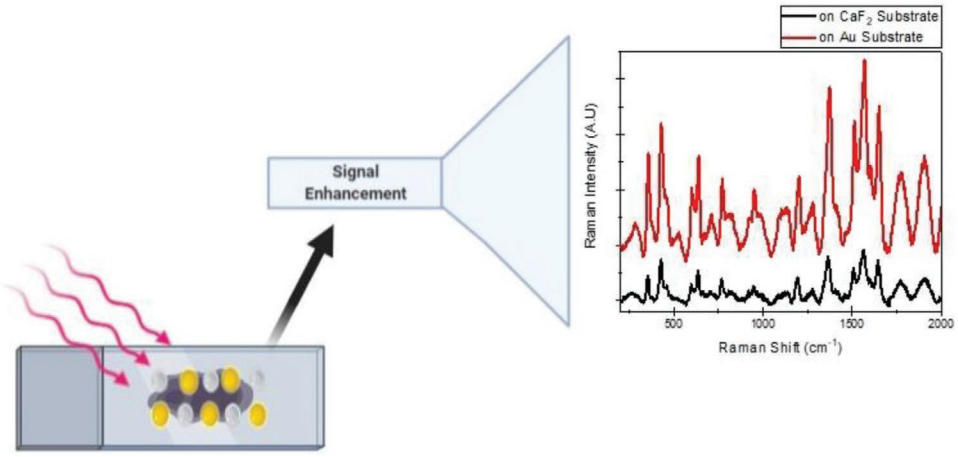

Figure 5. Signal enhancement due to the presence of silver (Ag) and gold (Au) NPs in close vicinity to the sample. Spectra show an increase in the intensity of rhodamine 123 peaks when it is positioned on AuNPs substrate.

Signal enhancement of Raman scattering can be achieved by bringing the sample into close vicinity to a nanostructured noble metal surface such as AuNPs and Ag NPs.[174] Although mechanisms of this enhancement is still a matter of debate, it can be obtained via two mechanisms: electromagnetic and chemical enhancement. Electromagnetic enhancement occurs as a result of surface plasmon polaritons (SPPs), which are formed when an electromagnetic wave travels along and has conductor metal–dielectric interference. SPPs are generated due to the combining of electromagnetic waves with the oscillating electron plasma of metals; only noble metals such as gold, silver, and copper favor the formation of plasmons. These increased local electromagnetic fields on the surface of metallic NPs are called "hot spots," and they increase the intensity of Raman scattering when they are close enough to the analyte. In addition to electromagnetic enhancement using SPR, chemical enhancement with a charge transfer between the metallic surface and analyte molecule can contribute to an increase in signal intensity. However, this mechanism is thought to be less effective than electromagnetic enhancement.[175]

Numerous studies focus on the fabrication of SERS substrates and optimizing their synthesis, size, and shape to achieve optimum enhancement. AgNPs and AuNPs have been widely used as SERS substrates. The methods of synthesis and the chemicals used to reduce metallic ions to NPs have a significant effect on SERS activity. For example, Mikac et al. synthesized AgNPs by using various reducing agents and tested their SERS activity. According to their results, the best Raman signal enhancement was achieved when AgNPs are synthesized by the citrate reduction method.[176]

The size and shape of the NPs also play a crucial role in the enhancement process. The size of NPs affects the surface area, and thus the formation of SPPs. In one study, the SERS activity of AuNPs with various sizes was assessed. The SERS spectra of 4-amino thiophenol (4-ATP) and 4-nitrothiophenol (4-NTP) were examined by using various sizes of AuNPs from 17 to 80 nm. According to their results, the best signal enhancement was observed with 50 nm AuNPs.[177] In addition to their size, the shape of NPs also has a considerable impact on the number of hot spots formed on the surface. Shapes such as rod,[178] star,[179] flower,[180] snowflake,[181] or even wrinkled[182] AuNPs have been tested to establish their SERS activity. The main conclusion of these studies is that roughness, such as branches in the nanoparticle structure, supports the localization of the electromagnetic field, which results in enhanced Raman signal intensity. An example for signal enhancement in the presence of Ag and Au NPs can be seen in **Figure 5**.

4.3. Confocal Raman Microscopy

Raman spectroscopy offers analysis and imaging along the *Z*-axis (depth) in addition to the lateral axis (*XY*) at high resolution (lateral resolution up to 250 nm and axial resolution up to 800 nm) when combined with a confocal microscope. The resolution depends on many parameters related to the instrumental setup; the numerical aperture and wavelength of incident light are important factors for the calculation of resolution. The nature of the sample also affects the resolution. The Raman spectra recorded for each 250 nm in x and y directions can be integrated over specific bands, giving a false-color image of the distribution of components in the sample.[183]

CRM is a versatile imaging technique that has many applications in various areas of research. Imaging biological samples through CRM has many benefits. It is not only a rapid and nondestructive technique but also provides information about the chemical composition of the sample during the production of the spatial maps.[184] CRM has been used in the analysis of fibers,[184,185] lipid bilayers,[33] plants,[186] human hair,[187] and even cells and cell compartments.[188,189] Morphological and chemical characterizations can be conducted at different layers by moving the laser focus deeper into the sample. This is termed as "optical sectioning" and is a noninvasive method of obtaining a sample profile in three dimensions.[190] Although CRM is a suitable method for constructing Raman images of samples consisting of many different components, as in biological systems, multivariate data analysis is generally required to distinguish overlapping bands.[183] The data analysis methods applied in the literature depend on the sample and the aim of the study. For example, Sharikova et al.

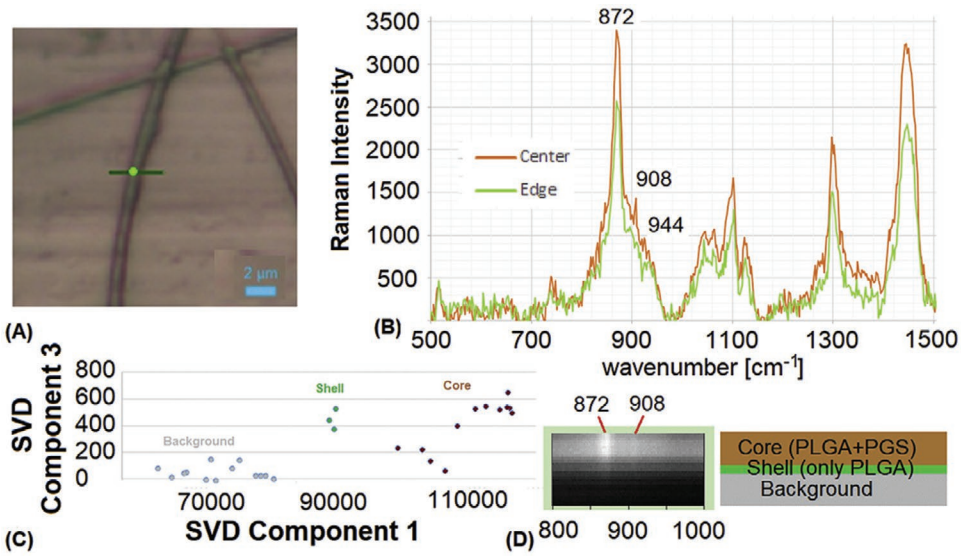

Figure 6. Raman spectroscopic imaging of a nanofiber: A) the optical image of the scanned nanofiber; B) spectra of nanofiber both from center and edge; C) SVD analysis; D) hyperspectral Raman image and the structure of the fiber-based on the SVD analysis. Reproduced with permission.[184] Copyright 2020, Elsevier.

characterized and analyzed a multicomponent nanofiber by using CRM. Characterizations of nanofibers that consist of different polymeric structures is important in tissue engineering applications. In this study, core/shell polyglycerol-sebacate/polylactic-*co*-glycolic acid (PGS/PLGA) nanofibers were prepared, and the distribution and thickness of each component were determined by plotting a 2D hyperspectral image based on the differences in the Raman spectra of PGS and PLGA, as shown in **Figure 6**. The contribution to the size of the diameter from core and shell parts can be measured by applying singular value decomposition (SVD) analysis to the hyperspectral image.[184] Similarly, Offroy et al. used a multivariate curve resolution (MCR-ALS) algorithm combined with a super-resolution approach to improving the spatial resolution of a far-field spectrometer. They tested their system on small aerosol particles and suggested that it can be used to monitor the physical and chemical processes that occur in the atmosphere.[191]

4.4. Stimulated Raman Scattering (SRS) Microscopy

SRS is a nonlinear optical process which provides higher sensitivity (μM to mM range), specificity, speed (0.1–10 s per frame), and spatial resolution (lateral: ≈300 nm, axial: 1–2 μm), properties that make it a useful tool in Raman imaging applications. This technique is obtained owing to two synchronized pulsed lasers (pump and Stokes beam); a selected molecular vibration is coherently excited by two beams, and when the frequency difference of the two beams is matched with the vibration frequency of the selected chemical bond, an enhancement in that specific Raman signal is obtained. The advantages of SRS microscopy mainly consist in being 1000-times faster than spontaneous Raman microscopy and in being nonaffected by the autofluorescence interference of the sample.[192] These improvements made SRS a preferable tool in imaging of biological samples. SRS microscopy coupled with small vibrational tags has been exploited to visualize nanoparticles in vitro and ex vivo,[193,194] to investigate drug uptake,[195] to analyze drug delivery through skin,[196] and study spatial distribution of specific molecules in order to understand their effect on cell death mechanisms.[197]

4.5. Raman Spectroscopy: Advantages over Other Techniques

The main advantage of spectroscopic and microscopic techniques is that they are rapid and enable the visualization of the sample. Raman spectroscopy combined with the confocal microscopy technique has benefits, as sample preparation steps such as staining[188] are not required, and as it is nondestructive it is suitable for working with living cells and tissues,[198] and is easily applicable to in vivo studies without any invasion of the human body.[187] In a recent study, the researchers measured the blood-sugar level from the skin surface without any invasive procedure. They used Raman spectroscopy to observe linear changes in glucose concentration, with a limit of detection (LoD) of 75 mg dL^{-1}, under the ear tissue of pigs.[199] Raman spectroscopy and imaging have also been applied in cancer diagnostics. One study consisted of testing two portable Raman devices on invasive ductal carcinoma (IDC) in the breast. The aim was to distinguish between healthy and cancerous cells by using the portable Raman probes during surgery, and the cancerous cells that had migrated from the tumor-site to the margins and transitional regions could thus be easily and rapidly detected. The Raman spectra were analyzed by principal component analysis combined with linear discriminant analysis (PCA-LDA), and the results showed that the transition from healthy to tumor tissue can be assessed more accurately using Raman spectroscopy.[200]

Another advantage of Raman spectroscopy, and particularly SERS, is that it can detect analytes at low concentrations. The design of new SERS substrates by using AgNPs was found to

increase the surface enhancement and the sensitivity of the method, which resulted in decreased LoD values of as low as 1×10^{-12} M for BSA.[201] These detection limits also led to the use of SERS as an immunoassay readout method involving Raman reporter molecules.[202]

4.6. Current Work on Raman Spectroscopy for the Study of Nanostructure Interaction with Biomolecules

As mentioned above, CRM is a promising analytical tool that has many benefits in the study of the diagnosis and treatment of diseases in vitro and in vivo. The properties of CRM make it useful in analysis of small molecule interactions. For example, Raman microscopy was used to show protein-ligand binding on porous silica-supported phospholipid bilayers. The differences in Raman peaks when the protein–ligand interaction takes place can be easily observed from the spectra.[33] In another study, the interaction of BSA–NP complexes with glycoprotein (gp60), which is present on the endothelial cell membrane and responsible for albumin transcytosis, was analyzed. Raman spectroscopy was one technique used to determine not only the affinity of BSA–NP complexes toward a different type of glycans but also the dominant binding sites of these complexes. The spectra of BSA, BSA–NP complexes, and BSA–NP complex with glycans were compared based on the main peaks of albumin such as amide I, tryptophan, tyrosine, and phenylalanine bands.[30] These studies demonstrate that Raman spectroscopy and CRM have a great potential for studies of nano–biointerfaces, as the changes in the vibrational modes of particles/biomolecules due to their chemical reactions or physical interactions can be identified.

Raman spectroscopy and SERS can be useful not only in terms of detection of proteins but also in the prediction of their conformation when they are attached to a surface. BSA, which is a widely used protein in scientific research, is commonly studied in investigations of the interactions of proteins with various nanomaterials. For example, Raman spectroscopy together with CD spectroscopy has been used to assess the spectral changes due to the interaction of BSA with MnO_2 NPs. In Raman spectra, structural information of proteins was obtained from the amide III region, phenylalanine, α-helix (C–C–N), tryptophan, and C–H bending bands. The intensities of these bands were compared before interaction with MnO_2 NPs (free BSA) and after the interaction (BSA + MnO_2). The decreases in these Raman peak intensities for free BSA after the conjugation was considered to be due to the loss of helicity of the protein.[31] Iosin et al. studied the interaction of BSA, which is the most abundant protein in blood plasma, with AuNPs of different shapes such as nanospheres and nanorods by using a combined study of fluorescence and SERS. The SERS spectrum of BSA adsorbed on AuNPs shows peaks related to specific bonds in the protein structure. In addition, these peak intensities may reveal the conformation of protein on the surface of the nanoparticle. For example, the peaks at 1005, 1446, and 1584 cm^{-1} were assigned to the phenyl aromatic ring and pyrrole ring breathing modes of tryptophan, and it was suggested that the high intensities of these peaks indicated that tryptophan residues were localized on the surface of the protein.[203] Similarly, Raman signals related to the vibrations of specific bonds can be used to understand the mechanistic of protein adsorption on the surface of NPs. For example, Treuel et al. investigated the adsorption of BSA on citrate-stabilized AgNPs by analyzing C—S and S—S bond vibrations. They compared Raman and SERS spectra of BSA and observed a strong decrease in S—S bond signal, and a strong enhancement in the C—S bond with a red-shift. These results indicate that C—S bonds in the protein structure are in close proximity of the AgNP surface and the red-shift in the wavenumber of these bonds results from the donation of electrons from free valances of sulfur to metal surface, which lowers the bond energy. In addition, to establish why the S–S signal decreases upon adsorption, the Raman and SERS spectra of cystine amino acid were analyzed. Very similar results were obtained for both, and it was concluded that the cleavage of S—S bonds in the protein structure is mainly the result of structural tensions due to the adsorption of BSA on the surface of the nanoparticle. The effect of a PVP coating on the adsorption process was also assessed. Depending on the dialysis and CD spectroscopy and Raman spectroscopy results, the authors concluded that the presence of a PVP coating around Ag and Au NPs prevents the strong interaction of the C—S bonds in the protein's structure with the surface of the metal.[32] A further study was conducted by the same group, in which protein–NP interactions were investigated by using insulin as the protein, due to the potential use of insulin coated AuNPs as drug carriers. SERS is used to observe changes in the secondary structure of insulin upon adsorption onto AuNPs. Raman and SERS spectra of insulin were compared, and it was shown that in addition to increasing the general signal intensity, due to the SPR in the presence of AuNPs, the enhancement of the Raman signal intensity of $-COO^-$ was found to be higher than the other peaks. The close interaction of the $-COO^-$ group with the surface of AuNPs can explain this and indicates that protein binding to the surface of NPs takes place through the electrostatic interaction between negatively charged carboxyl groups and the positively charged Au surface. This binding affects the secondary structure of insulin, and the changes in C—S and S—S bond-stretching regions revealed the loss of the secondary structure.[204]

The conformational changes due to the adsorption on AuNPs can be used to differentiate two proteins with similar structures. Binding sites of BSA and HSA have been determined by comparing the Raman and SERS spectra of both proteins. Selective enhancement of specific bands makes it possible to understand which amino acid sequences are close to AuNPs during the interaction process. In addition, the presence of bands related to nonpolar residues such as phenylalanine and tryptophan can be an indication of the disturbed secondary structure of proteins due to interaction with AuNPs. For BSA molecule, SERS spectra suggest that most of the electrostatic interaction occurs between citrate ligands on the surface of AuNPs and lysine residues of the protein. The same phenomenon is also valid for HSA; however, the spectra of HSA also contain stretching vibrations of $-COO^-$ groups. According to the authors, this difference is due to the deprotonation of the $-COO^-$ group, as the local microenvironment of amino acid side chains is affected by neighboring residues. The small differences in the primary structure may result in different binding patterns, even

for proteins that have a 77.5% sequence similarity. Thus, SERS with high selectivity and sensitivity can be used to detect and distinguish proteins that are almost identical, and thus represents a promising tool in the characterization of nano–biointeractions.[205] Raman spectral bands of tryptophan residues can be very useful for understanding the effects of NPs on the protein structure in various environments. Gambucci et al. investigated the interaction of Gramicidin A (Gram A) peptide and dodecanethiol-stabilized silver NPs (D-AgNPs) with hydrophobic coating, mainly based on IR and Raman spectroscopy. The position and function of Gram A peptide were investigated in POPC liposomes as Gram A is a model for membrane proteins. Membrane proteins have an important role in cellular trafficking, which mainly depend on protein conformations. In this study, the changes in four marker tryptophan Raman bands, which originated from the indole ring in its structure, were used. Raman intensities and shifts in these bands showed the orientation of the peptide in POPC liposomes both in the presence of D-AgNPs and without. The characteristics of the Raman peaks in the region of 730–810 cm^{-1} are sensitive to the local environment of tryptophan, as they are attributed to the ring breathing mode of the indole group. This vibrational mode shows a Raman signal of around 760 cm^{-1}. Unfolding of protein and exposure of tryptophan residues to the aqueous environment in POPC and POPC/D-AgNPs systems results in a decrease in the intensity of this signal and the formation of a second Raman peak at around 780 cm^{-1}. The differences in the other characteristic Raman peaks of indole at 880 cm^{-1} and a doublet at 1360 and 1340 cm^{-1} in various environments also suggested that D-AgNPs cause a change in the conformation of the peptide, which increases the exposure of tryptophan residues to the aqueous environment.[206]

In addition to conformational changes of proteins, SERS can be a useful tool for similar purposes, such as detecting conformational changes of aptamers when they are exposed to a target molecule. Neumann et al. used two aptamers that are specific to a protein, which is a platelet-derived growth factor (PDGF-BB), and a small molecule, which is cocaine. Molecules that are nonspecific to these aptamers are used for comparison. To obtain surface enhancement, gold nanoshells were used as a substrate. Aptamer molecules were thermally treated and formed a self-assembled monolayer on Au nanoshells, as they were thiolated on one terminus. Covalent binding of aptamers on the nanoshell substrate led to highly reproducible SERS spectra. However, interaction with the target molecule causes conformational changes in the structure of the aptamer, and this led to a decrease in reproducibility of SERS spectra compared to the spectra of aptamers before exposure to the target molecule. The changes in the SERS spectra with the addition of target/nontarget molecules were quantified by using a spectral cross-correlation function, and the results were verified by correlating with CD spectroscopy. The anti-PDGF aptamer demonstrated a high specificity toward its target molecule, as the reproducibility of spectra was reduced by the addition of the target molecule, but it did not change when incubated with a control protein. However, it was observed that the reproducibility of the SERS spectra of the anticocaine aptamer changed due to incubation in terms of not only its target molecule, cocaine, but also other molecules like benzocaine and caffeine. Overall, the results indicate that SERS can also be used for the assessment of the specificity of aptamers for their target molecules.[207] Similarly, Dekhili et al. used Raman spectroscopy to understand the interaction of aptamers with their target protein under two different conformations and various concentrations. First, they investigated how different grafting methods affect the conformation of the Cu, Zn superoxide dismutase (SOD 4) aptamer on diacid pegylated gold NPs (PEG-AuNPs). They compared the Raman signals of PEG-AuNPs functionalized with SOD 4 aptamer (APT) by using either 1-ethyl-3-(3-dimethylaminopropyl)carbodiimide/N-hydroxysuccinimide (EDC/NHS) chemistry or complexation reaction. The interaction of SOD 4 (at different concentrations) with aptamer in the two conformations was then studied using Raman spectroscopy. The appearance of amide II (1587–1620 cm^{-1}) and amide III (1200–1300 cm^{-1}) bands and also a signal associated with C–C vibrations of tripeptide (934 cm^{-1}) confirmed the interaction of APT and SOD 4. Other changes in Raman spectra that confirm the protein–aptamer interaction are the enhancement of 2880, 2936, and 2965 cm^{-1} bands, which are characteristic bands of C–H and O–H stretching vibrations, and the presence of the vibration of the amine group at 1450 cm^{-1}. The effect of protein concentration on the interaction was evaluated by comparing various Raman signals, and two specific Raman peaks of SOD 4: 748 and 940 cm^{-1} for the EDC/NHS method and 735 and 928 cm^{-1} for the complexation method. These were used to calculate the LODs and were found to be 8×10^{-9} and 2×10^{-9} M, respectively.[208]

The study of Barkhade et al. is another example of using Raman spectroscopy to investigate the interaction of NPs with biomolecules at the nano–biointerface. Titanium dioxide NPs (TiO_2 NPs) were selected, as they are widely used in daily products such as pharmaceuticals, papers, textiles, plastics, and cosmetics. Their interactions with adenosine triphosphate (ATP) molecule were investigated, as ATP is the currency of energy in the cell and is a molecule likely to interact with NPs when they enter into the cells. They used two complementary spectroscopic techniques, Raman and FTIR spectroscopy, and TEM for both the characterization of iron-incorporated titanium dioxide NPs (Fe content TiO_2 NPs) and their interaction with the ATP molecule. It was expected that Fe incorporation would minimize the toxic effect of TiO_2 by changing the particle–matrix and parent particle dissolution rate. The spectra of pure and hydrolyzed ATP, and the spectra after their interaction with Fe content TiO_2 NPs with varying amounts of Fe, were obtained. The Raman spectrum of ATP mainly consists of three moieties: adenine, phosphate, and ribose. The peaks related to these moieties were used to understand the structural changes due to the interaction of Fe in the TiO_2 matrix. The formation of new peaks with an increasing amount of Fe in the nanoparticle composition showed that the presence of Fe contributes to the coordination sites of NPs and results in a stronger interaction between the nanoparticle and ATP molecules.[209]

As mentioned above, Raman spectroscopy is advantageous in terms of studying living organisms such as cells. It enables investigations at the single-cell level, which makes it a convenient method for studying nanoparticle uptake and monitoring their accumulation within the cell compartments, without any necessity for labeling. CRM was used to demonstrate the

colocalization of carbon nanotubes (CNTs), aluminum oxide (Al_2O_3), and cerium dioxide (CeO_2) NPs in hepatocarcinoma cell compartments. The spectra of three different cell compartments (lipid bodies, cytoplasm, and nucleus) were recorded after exposing cells to CeO_2 NPs. These three spectra were used to differentiate between compartments, depending on their Raman signal from CH_2, CH_3 symmetric stretching bands, amide I and amide III bands, CH deformation modes of proteins, and vibrations related to nucleobases such as adenine and guanine. In order to understand the effect of coating, the surface of CNT was coated with either lipids or poly-sulfo propyl methacrylate (PSPM). By taking the Raman spectra of hepatocarcinoma cells after exposing them to the NPs and analyzing the spectra, they found that CeO_2 NPs were distributed in the cytoplasm along with Al_2O_3, which is mainly accumulated in protein-rich regions close to the nucleus. They also showed that the surface properties have an important role in the distribution of NPs, as lipid-coated CNT is mainly found close to lipid bodies, whereas CNT coated with PSPM avoided lipid-rich regions in the cell.[189] In a recent study, Raman spectroscopy combined with optical tweezers was used to understand the effect of Ag and Au NPs on living human red blood cells (RBCs). Variations in the Raman spectra were observed, due to different sizes and concentrations of NPs. The spectral changes, particularly the change in the peak ratio of 1224–1211 cm^{-1}, was monitored as this indicates the hemoglobin oxygenation status inside the cells in the presence of Ag and Au NPs.[210]

Raman spectroscopy and imaging are also helpful techniques for tracking the NPs inside the cells, which makes it a preferable method for monitoring drug delivery systems. Generally, chemical tags that give a Raman signal in the cell-silent region (1800–2800 cm^{-1}) are used when designing nanocarriers, to distinguish the signal coming from the nanocarrier and to avoid background signals coming from the cell.[211] For example, two chemical tags (alkyne and deuterium) were used to label PLGA, which is an FDA-approved, biocompatible, and biodegradable polymer generally used in drug delivery research. In this study, SRS microscopy was used for imaging NPs in cultured microglia and in ex vivo brain tissue. Recording images with SRS instead of spontaneous Raman scattering enables the probing of a specific vibrational bond by using two lasers, and it is more advantageous in terms of signal intensity and image acquisition speed when compared to spontaneous Raman scattering. **Figure 7** shows that CH_3 vibrations at 2939 cm^{-1} and CH_2 vibrations at 2856 cm^{-1} belong to the protein and cellular lipid content of microglia cells, respectively. To visualize the location of PLGA NPs inside cells, a C–D vibration at 2253 cm^{-1} was used for deuterated PLGA (PLGA-D) and C≡C vibration at 2128 cm^{-1} was used for alkyne tagged PLGA (PLGA-alkyne). In vitro studies revealed that alkyne tags have a stronger signal, and thus

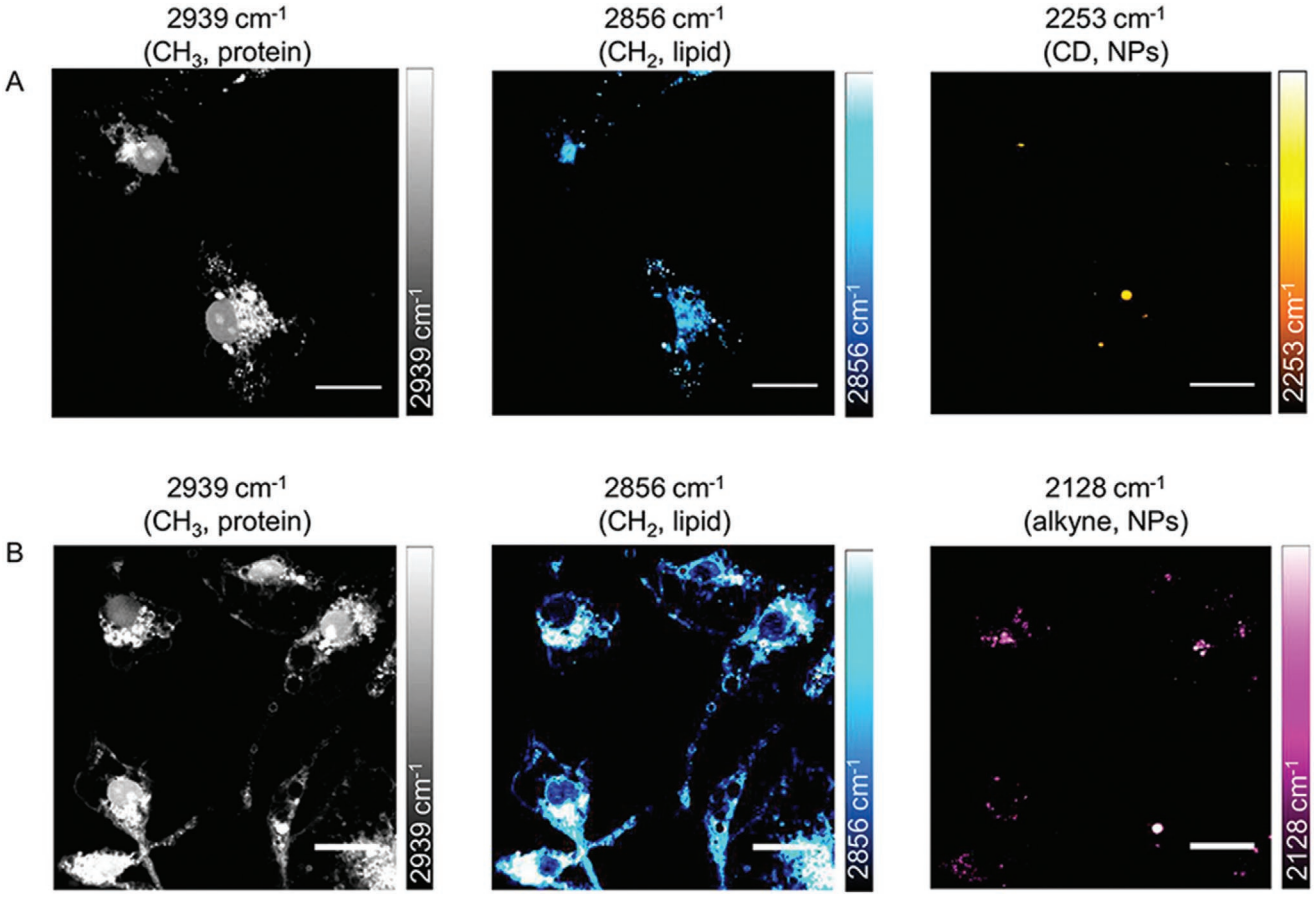

Figure 7. SRS imaging of polymeric NPs tagged with A) deuterium and B) alkyne after 24 h of incubation with microglia cells. Reproduced under the terms of a Creative Commons Attribution (CC-BY) License.[194] Copyright 2019, American Chemical Society.

only alkyne-tagged NPs were used in ex vivo studies. Mouse brain slices were treated with NPs and SRS imaging was used to investigate the uptake of NPs. SRS imaging along with the immunofluorescence technique and a Z-stack analysis showed that NPs were internalized by microglia cells, but the internalization was not as homogenous as in in vitro microglia cultures.[194]

The same technique was also used to investigate the delivery of ketoprofen and ibuprofen in propylene glycol through intact and porated porcine skin. Either the drug itself or the solution (propylene glycol) were deuterated and C—D bond vibration was used to distinguish signals related to drugs from the CH_2 signal of the skin. This contrast was used to construct 3D images of skin surface treated with drugs and makes it possible to understand the transport mechanisms and changes in the structure of both drugs and the skin structure.[196] Similarly, SRS was used to determine the contribution of dissolution in the biokinetics of insoluble barium sulfate NPs ($BaSO_4$ NPs) and their translocation in several tissues such as lungs, bone, liver, spleen, and kidneys of rats after 28 days of their intratracheal instillation. As a control experiment, the same procedure was also applied using barium chloride ($BaCl_2$), which is a soluble salt of barium. The selected region of interest from lung and bone tissues and their Raman spectra is given in **Figure 8**. The specific Raman peak of $BaSO_4$ is at 980 cm^{-1}, and Raman spectra were analyzed to detect the presence of intact $BaSO_4$ in the aforementioned tissue samples. This peak can be detected only in several foci in the lungs, and did not appear in the other tissues such as bone nor in $BaCl_2$ instilled lungs, which indicated that intact $BaSO_4$ NPs are not translocated in extrapulmonary organs.[193]

These studies show that Raman and Raman-related analysis methods have great potential for in vivo studies, and thus are promising tools for monitoring the effects of drugs and the drug delivery systems throughout the body. One problematic aspect of in vivo studies is the formation of so-called BC around NPs when they are administrated into living systems. This corona changes the surface properties of NPs and defines a new biological identity. The adsorption of proteins or other biomolecules on the surface of NPs can block the binding sites or may lead to an in vivo response.[212] In addition, it is important to understand the effects of nanoparticle conjugation on the structure and function of proteins for bioinspired applications. Raman spectroscopy is one tool that can provide insights in terms of the formation mechanism of BC. Thus, the interaction of an enzyme, lysozyme (Lys), with nitrogen-doped reduced graphene oxide (NrGO) covered with AuNPs on its surface has been investigated. Among many other techniques, Raman spectroscopy revealed that Lys interacts with the surface through S—S stretching bonds in the Cys residues.[213] The plasmonic properties of AuNPs make them appropriate probes for studying BC formation in various environments. AuNPs increase the Raman signal intensity of the residues that are close to their surfaces. This enhancement was used to establish which residues in the structure of BSA interact with AuNPs surface at varying concentrations.[214] In addition, the recent study by Szekeres et al. showed that SERS is a promising tool for observing specific nanoparticle–biomolecule interactions even in vivo studies. In this study, the SERS spectra of the endolysosomal environment of live cells were compared with cytoplasmic extracts after both samples were incubated with AuNPs. The aim was to establish how the active processing of NPs in the living cells affects the BC formation and fragmentation by comparing relative occurrences of specific protein vibrations. The data analysis showed that the occurrences of bands associated with C–S, S–S stretching vibrations, and signals of nonpolar side chains were greater in the spectra of endolysosomes, whereas the amide bands indicating the polypeptide backbone were lower in terms of the spectra of isolated cytoplasm. This led to the fragmentation of intact proteins after their adsorption on the nanoparticle surface, instead of the direct adsorption of protein products that have already been cleaved. To support this, the fragmentation of a model protein was examined by obtaining the spectra of BSA, trypsin, and trypsinized BSA.[215] In another study, SERS tags that consist of spherical AuNPs as the plasmonic core, small cyclic arginine-glycine-aspartic acid-phenylalanine-cysteine (RGDFC) peptide as a protective coating and biorecognition element, and 4-mercaptobenzonitrile (MBN) as a Raman reporter molecule were used to target $\alpha_v\beta_3$ integrins on human metastatic colon cancer cells. These SERS tags were designed to be used in fixed/live-cell experiments, and thus they can test whether a BC is formed around NPs in cell culture conditions such as cell media supplemented with fetal bovine serum (FBS). FBS has a high number of growth factors, so it is often used in cell media to enhance the survival and growth of cells. To demonstrate the effect of FBS on the formation of the BC, bare AuNPs were treated with both RPMI cell media and FBS supplemented RPMI media. SERS was used to assess the difference between the formation of BCs on AuNPs under various environmental conditions. According to the SERS results, the composition of the BC formed around the surface of AuNPs differed depending on the presence of FBS. In FBS-free cell media, amino acids are electrostatically adsorbed on the surface, whereas FBS brings the large proteins, which are adsorbed on the AuNPs surface instead of small amino acids. This difference can be seen in the spectra; the large proteins have poor scattering properties and fluoresce, which hides the Raman signal. However, SERS peaks of small amino acids on the surface of AuNPs can be observed when FBS-free media is used. To prevent the formation of the corona, the small cyclic peptide was grafted on AuNPs. In terms of its size and the zeta potential results, Au–RGDFC–MBN can retain a negative charge on the surface and showed only a small increase in size. As the Raman reporter molecule was not blocked by the BC, the SERS tags could be used to probe $\alpha_v\beta_3$ integrins on the surface of the human metastatic cell line. By following the main peaks of MBN, the clusters of integrin could be detected on the cell membrane.[216] A summary of current applications of Raman spectroscopy/microscopy in bio-related studies is listed in **Table 1**.

5. Conclusions

We have presented the current state of the art in BC studies, and described how BCs can affect nanostructure interaction with biological systems, the parameters that affect BCs, and how BCs can be used in biomedical approaches. Raman

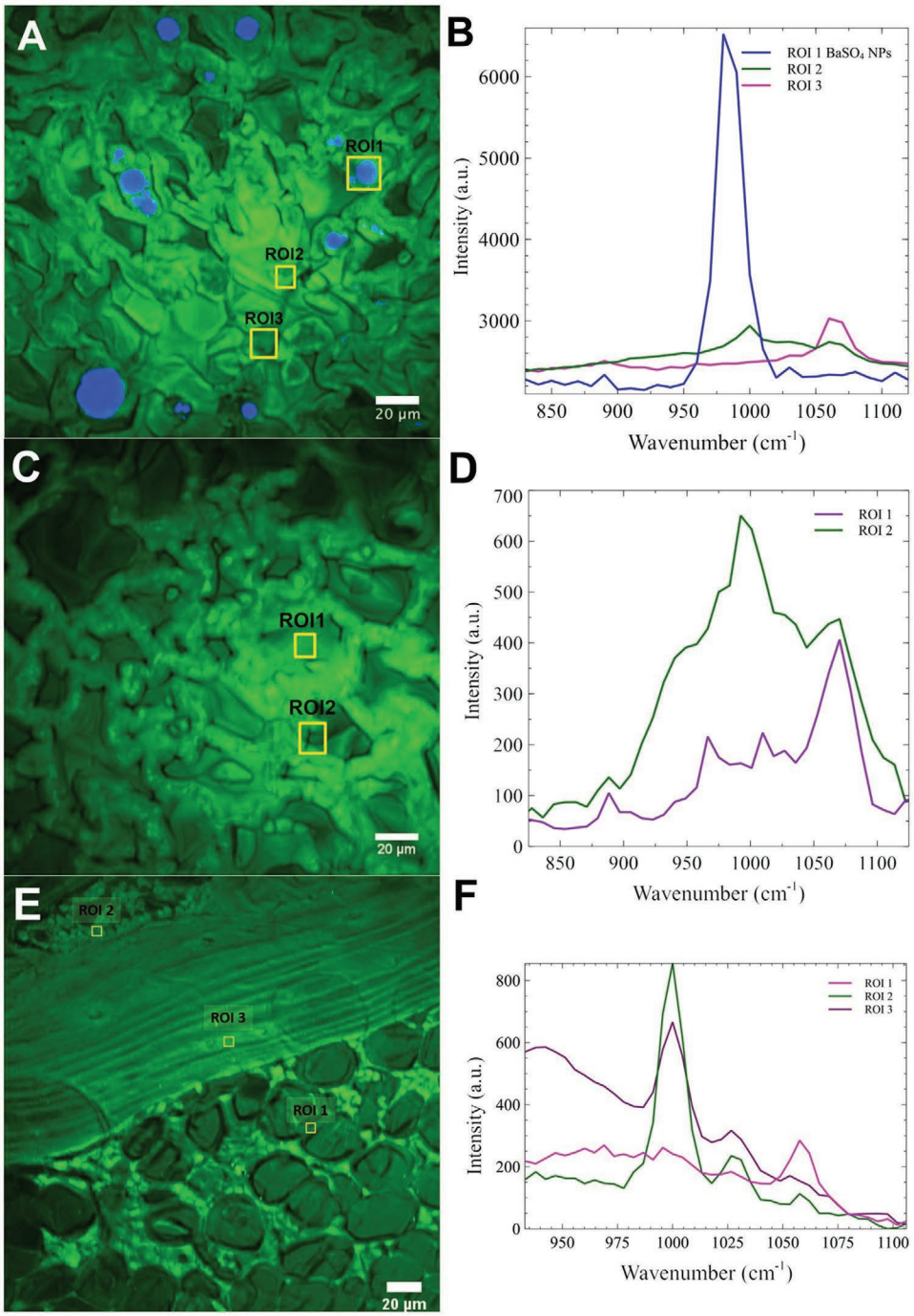

Figure 8. SRS microscopic examination of lungs and bone 28 days after intratracheal instillation of 50 mg kg^{-1} $BaSO_4$ NPs. Images and related spectra of regions of interest in A,B) lungs of rats instilled with $BaSO_4$ NPs, which are indicated by blue areas, C,D) lungs of rats instilled with ionic $BaCl_2$, and E,F) bones of rats instilled with $BaSO_4$ NPs. Reproduced under the terms of the Creative Commons CC-BY License.[193] Copyright 2019, The Authors.

spectroscopy, and in particular Raman microscopy, represents a potentially disruptive tool for the study of BC–nanostructure complexes, as it enables BC analysis without the need of staining with high spatial resolution. Information about both the protein components of BCs and other biological molecules like oligonucleotides and lipids can thus be obtained. Currently, the biggest limitation of Raman-based approaches is represented by the poor signal/noise ratio typical of the Raman scattering when compared to other imaging techniques like fluorescence-based approaches. However, as we discussed in the main text, the use of techniques like SERS imaging can greatly enhance the signal/noise ratio, improving both the resolution and the acquisition speed. As previously mentioned, Raman imaging is currently less used in BC studies

Table 1. Current applications of Raman spectroscopy and microscopy in biorelated studies.

Investigation	Technique	NP/biomolecule	Aim	Refs.
Protein biosensing	CRM	BSA–AgNPs–glycans	Understanding interaction between albumin–NP conjugate with glycans	[30]
Protein biosensing	CRM	Mannose–concanavalin A binding at porous silica-supported phospholipid bilayers	Investigation of porous silica-supported phospholipid bilayers as a platform for label-free detection of protein–ligand interactions	[33]
Protein–NP interactions	SERS	BSA–AuNPs	Characterization of binding properties between proteins and NPs	[203]
Protein–NP interactions	SERS	BSA–AuNPs BSA–AgNPs (citrate stabilized and PVP coated)	Effect of PVP coating on the mechanistic of protein adsorption onto NPs surface	[32]
Protein–NP interactions	SERS	Insulin–AuNPs	Understanding changes in protein structure upon adsorption onto a metallic surface	[204]
Protein–NP interactions	SERS	BSA–AuNPs HSA–AuNPs	Differences in adsorption mechanism of BSA and HSA	[205]
Peptide–NP interactions	SERS	Gram A–D-AgNPs (in ethanol and in phospholipid membrane)	Effect of D-AgNPs on the conformation and function of a model membrane protein	[206]
Protein–NP interactions	Raman spectroscopy	BSA–MnO_2	Understanding the impact of NPs on the structure of BSA	[31]
Enzyme–NP interactions	Raman spectroscopy	Au(0)–NrGO–Lys	Studying various types of biomolecular interactions at nano–biointerface	[213]
Biomolecule–NP interactions	SERS	BSA–AuNPs DNA–AuNPs	SERS probing in biomolecular solutions	[214]
Aptamer–analyte interactions	SERS	Anti-PDGF–PDGF Anticocaine–Cocaine	Detecting conformational changes due to aptamer–analyte interaction	[207]
Aptamer–analyte interactions	SERS	SOD 4–APT in PEG-AuNPs SOD 4–APT on PEG-AuNPs	The effect of grafting method on the interaction between aptamer and SOD 4 glycoprotein	[208]
Nanoparticle–biomolecule interactions	Raman spectroscopy	ATP–TiO_2 NPs ATP–Fe content TiO_2 NPs	Understanding the effect of Fe content on the interaction between TiO_2 NPs and ATP	[209]
BC studies	SERS	Endolysosome–AuNPs Isolated cytoplasm–AuNPs BSA–AuNPs Trypsin–AuNPs Trypsinized BSA–AuNPs	Effect of active processing on intracellular BC and the corresponding protein–NP interactions	[215]
Raman imaging	SRS microscopy	Visualization of specific molecules, NPs, or drugs	Enhancement in specific Raman signal of biomolecules, NPs, and/or Raman active tags for imaging purposes	[194,196,193]

with respect to other techniques. In order to fill this gap, future efforts should aim toward the combination of Raman imaging with other complementary techniques to study the impact of BC on nanomaterial properties, its effect on nanomaterial/cell interactions, and the bioexploitability of BC. We do not envision that Raman microscopy can completely replace other techniques, but we are confident that its complementary use, alongside other approaches discussed in this work, will provide new insights and information that will be of pivotal importance for understanding and applying the interaction between nanostructures and biological environments.

Conflict of Interest

The authors declare no conflict of interest.

Keywords

biomolecular corona, nanostructures, protein corona, Raman microscopy, Raman spectroscopy

Received: June 2, 2021
Revised: August 11, 2021
Published online: September 4, 2021

Acknowledgements

M.B. and M.B.G. contributed equally to this work.
Open access funding enabled and organized by Projekt DEAL.

[1] T. Lima, K. Bernfur, M. Vilanova, T. Cedervall, *Sci. Rep.* **2020**, *10*, 1129.
[2] S. Wan, P. M. Kelly, E. Mahon, H. Stöckmann, P. M. Rudd, F. Caruso, K. A. Dawson, Y. Yan, M. P. Monopoli, *ACS Nano* **2015**, *9*, 2157.

[3] S. Xu, S. Hossaini Nasr, D. Chen, X. Zhang, L. Sun, X. Huang, C. Qian, *ACS Biomater. Sci. Eng.* **2018**, *4*, 654.
[4] S. Kihara, N. J. van der Heijden, C. K. Seal, J. P. Mata, A. E. Whitten, I. Köper, D. J. McGillivray, *Bioconjugate Chem.* **2019**, *30*, 1067.
[5] S. Dominguez-Medina, L. Kisley, L. J. Tauzin, A. Hoggard, B. Shuang, A. S. D. S. Indrasekara, S. Chen, L.-Y. Wang, P. J. Derry, A. Liopo, E. R. Zubarev, C. F. Landes, S. Link, *ACS Nano* **2016**, *10*, 2103.
[6] D. Baimanov, J. Wu, R. Chu, R. Cai, B. Wang, M. Cao, Y. Tao, J. Liu, M. Guo, J. Wang, X. Yuan, C. Ji, Y. Zhao, W. Feng, L. Wang, C. Chen, *ACS Nano* **2020**, *14*, 5529.
[7] E. Casals, T. Pfaller, A. Duschl, G. J. Oostingh, V. F. Puntes, *Small* **2011**, *7*, 3479.
[8] J. Y. Oh, H. S. Kim, L. Palanikumar, E. M. Go, B. Jana, S. A. Park, H. Y. Kim, K. Kim, J. K. Seo, S. K. Kwak, C. Kim, S. Kang, J.-H. Ryu, *Nat. Commun.* **2018**, *9*, 4548.
[9] C. Rodriguez-Quijada, H. de Puig, M. Sánchez-Purrà, C. Yelleswarapu, J. J. Evans, J. P. Celli, K. Hamad-Schifferli, *ACS Appl. Mater. Interfaces* **2019**, *11*, 14588.
[10] Z. Wang, C. Wang, S. Liu, W. He, L. Wang, J. Gan, Z. Huang, Z. Wang, H. Wei, J. Zhang, L. Dong, *ACS Nano* **2017**, *11*, 1659.
[11] G. Su, H. Jiang, B. Xu, Y. Yu, X. Chen, *Mol. Pharmaceutics* **2018**, *15*, 5019.
[12] R. Cai, J. Ren, Y. Ji, Y. Wang, Y. Liu, Z. Chen, Z. Farhadi Sabet, X. Wu, I. Lynch, C. Chen, *ACS Appl. Mater. Interfaces* **2020**, *12*, 1997.
[13] M. delPilar Chantada-Vázquez, A. C. López, M. G. Vence, S. Vázquez-Estévez, B. Acea-Nebril, D. G. Calatayud, T. Jardiel, S. B. Bravo, C. Núñez, *J. Proteomics* **2020**, *212*, 103581.
[14] J. F. Affonso de Oliveira, F. R. Scheffer, R. F. Landis, É. Teixeira Neto, V. M. Rotello, M. B. Cardoso, *ACS Appl. Mater. Interfaces* **2018**, *10*, 41917.
[15] A. Solorio-Rodríguez, V. Escamilla-Rivera, M. Uribe-Ramírez, A. Chagolla, R. Winkler, C. M. García-Cuellar, A. De Vizcaya-Ruiz, *Nanoscale* **2017**, *9*, 13651.
[16] Z. Liu, X. Zhan, M. Yang, Q. Yang, X. Xu, F. Lan, Y. Wu, Z. Gu, *Nanoscale* **2016**, *8*, 7544.
[17] H. Zhang, J. Peng, X. Li, S. Liu, Z. Hu, G. Xu, R. Wu, *Colloids Surf., B* **2018**, *167*, 220.
[18] L. Landgraf, C. Christner, W. Storck, I. Schick, I. Krumbein, H. Dähring, K. Haedicke, K. Heinz-Herrmann, U. Teichgräber, J. R. Reichenbach, W. Tremel, S. Tenzer, I. Hilger, *Biomaterials* **2015**, *68*, 77.
[19] J. Zhao, S. Wu, J. Qin, D. Shi, Y. Wang, *ACS Appl. Mater. Interfaces* **2018**, *10*, 41986.
[20] Z. Zhang, C. Wang, Y. Zha, W. Hu, Z. Gao, Y. Zang, J. Chen, J. Zhang, L. Dong, *ACS Nano* **2015**, *9*, 2405.
[21] Q. Yu, L. Zhao, C. Guo, B. Yan, G. Su, *Front. Bioeng. Biotechnol.* **2020**, *8*, 210.
[22] H. Yang, C. Hao, Z. Nan, R. Sun, *Int. J. Biol. Macromol.* **2020**, *155*, 208.
[23] K. Natte, J. F. Friedrich, S. Wohlrab, J. Lutzki, R. von Klitzing, W. Österle, G. Orts-Gil, *Colloids Surf., B* **2013**, *104*, 213.
[24] H. Yang, M. Wang, Y. Zhang, X. Liu, S. Yu, Y. Guo, S. Yang, L. Yang, *Int. J. Biol. Macromol.* **2019**, *135*, 1114.
[25] N. M. Meghani, H. Amin, C. Park, J.-H. Cui, Q.-R. Cao, K. H. Choi, B.-J. Lee, *Mater. Sci. Eng., C* **2020**, *111*, 110760.
[26] V. Mirshafiee, R. Kim, S. Park, M. Mahmoudi, M. L. Kraft, *Biomaterials* **2016**, *75*, 295.
[27] R. Safavi-Sohi, S. Maghari, M. Raoufi, S. A. Jalali, M. J. Hajipour, A. Ghassempour, M. Mahmoudi, *ACS Appl. Mater. Interfaces* **2016**, *8*, 22808.
[28] A. Selva Sharma, M. Ilanchelian, *J. Phys. Chem. B* **2015**, *119*, 9461.
[29] L. Zedler, M. D. Hager, U. S. Schubert, M. J. Harrington, M. Schmitt, J. Popp, B. Dietzek, *Mater. Today* **2014**, *17*, 57.
[30] N. Kumari, V. L. Mathe, P. M. Dongre, *Int. J. Biol. Macromol.* **2019**, *126*, 74.
[31] A. Baral, L. Satish, D. P. Das, H. Sahoo, M. K. Ghosh, *New J. Chem.* **2017**, *41*, 8130.
[32] L. Treuel, M. Malissek, S. Grass, J. Diendorf, D. Mahl, W. Meyer-Zaika, M. Epple, *J. Nanopart. Res.* **2012**, *14*, 1102.
[33] D. A. Bryce, J. P. Kitt, J. M. Harris, *J. Am. Chem. Soc.* **2018**, *140*, 4071.
[34] Y. T. Ho, N. A. Azman, F. W. Y. Loh, G. K. T. Ong, G. Engudar, S. A. Kriz, J. C. Y. Kah, *Bioconjugate Chem.* **2018**, *29*, 3923.
[35] R. delCaño, L. Mateus, G. Sánchez-Obrero, J. M. Sevilla, R. Madueño, M. Blázquez, T. Pineda, *J. Colloid Interface Sci.* **2017**, *505*, 1165.
[36] J. H. Shannahan, R. Podila, J. M. Brown, *Int. J. Nanomed.* **2015**, *10*, 6509.
[37] S. Lara, A. Perez-Potti, L. M. Herda, L. Adumeau, K. A. Dawson, Y. Yan, *ACS Nano* **2018**, *12*, 4930.
[38] J. Ren, R. Cai, J. Wang, M. Daniyal, D. Baimanov, Y. Liu, D. Yin, Y. Liu, Q. Miao, Y. Zhao, C. Chen, *Nano Lett.* **2019**, *19*, 4692.
[39] N. Kaur, P. Mathur, P. Yadav, S. Chakraborty, A. Shanavas, *Carbohydr. Polym.* **2020**, *237*, 116170.
[40] J. Beurton, P. Lavalle, A. Pallotta, T. Chaigneau, I. Clarot, A. Boudier, *Int. J. Pharm.* **2020**, *580*, 119244.
[41] D. J. Sobczynski, O. Eniola-Adefeso, *Acta Biomater.* **2017**, *48*, 186.
[42] L. Digiacomo, F. Cardarelli, D. Pozzi, S. Palchetti, M. A. Digman, E. Gratton, A. L. Capriotti, M. Mahmoudi, G. Caracciolo, *Nanoscale* **2017**, *9*, 17254.
[43] W. Lai, D. Li, Q. Wang, X. Nan, Z. Xiang, Y. Ma, Y. Liu, J. Chen, J. Tian, Q. Fang, *Int. J. Nanomed.* **2020**, *15*, 1481.
[44] R. Liu, W. Jiang, C. D. Walkey, W. C. W. Chan, Y. Cohen, *Nanoscale* **2015**, *7*, 9664.
[45] C. C. Fleischer, C. K. Payne, *Acc. Chem. Res.* **2014**, *47*, 2651.
[46] K. Kristensen, T. B. Engel, A. Stensballe, J. B. Simonsen, T. L. Andresen, *J. Controlled Release* **2019**, *307*, 1.
[47] H. Wang, K. Dardir, K.-B. Lee, L. Fabris, *Bioconjugate Chem.* **2019**, *30*, 2555.
[48] H. de Puig, I. Bosch, M. Carré-Camps, K. Hamad-Schifferli, *Bioconjugate Chem.* **2017**, *28*, 230.
[49] S. B. Subramaniyan, S. Vijayakumar, S. Megarajan, R. K. Kamlekar, V. Anbazhagan, *ACS Omega* **2019**, *4*, 14049.
[50] D. K. Ban, S. Paul, *Colloids Surf., B* **2016**, *146*, 577.
[51] S. Palchetti, L. Digiacomo, F. Giulimondi, D. Pozzi, G. Peruzzi, G. Ferri, H. Amenitsch, F. Cardarelli, M. Mahmoudi, G. Caracciolo, *Biochim. Biophys. Acta, Biomembr.* **2020**, *1862*, 183159.
[52] D. Zhu, H. Yan, Z. Zhou, J. Tang, X. Liu, R. Hartmann, W. J. Parak, N. Feliu, Y. Shen, *Biomater. Sci.* **2018**, *6*, 1800.
[53] E. Quagliarini, R. Di Santo, S. Palchetti, G. Ferri, F. Cardarelli, D. Pozzi, G. Caracciolo, *Pharmaceutics* **2020**, *12*, 113.
[54] J. L. Betker, J. Gomez, T. J. Anchordoquy, *J. Controlled Release* **2013**, *171*, 261.
[55] L. Digiacomo, D. Pozzi, H. Amenitsch, G. Caracciolo, *Biomater. Sci.* **2017**, *5*, 1884.
[56] M. J. Hajipour, J. Raheb, O. Akhavan, S. Arjmand, O. Mashinchian, M. Rahman, M. Abdolahad, V. Serpooshan, S. Laurent, M. Mahmoudi, *Nanoscale* **2015**, *7*, 8978.
[57] A. Nandakumar, Y. Xing, R. R. Aranha, A. Faridi, A. Kakinen, I. Javed, K. Koppel, E. H. Pilkington, A. W. Purcell, T. P. Davis, P. Faridi, F. Ding, P. C. Ke, *Biomacromolecules* **2020**, *21*, 988.
[58] E. H. Pilkington, Y. Xing, B. Wang, A. Kakinen, M. Wang, T. P. Davis, F. Ding, P. C. Ke, *Sci. Rep.* **2017**, *7*, 2455.
[59] E. H. Pilkington, O. J. R. Gustafsson, Y. Xing, J. Hernandez-Fernaud, C. Zampronio, A. Kakinen, A. Faridi, F. Ding, P. Wilson, P. C. Ke, T. P. Davis, *ACS Nano* **2018**, *12*, 6066.
[60] K. Ezzat, M. Pernemalm, S. Pålsson, T. C. Roberts, P. Järver, A. Dondalska, B. Bestas, M. J. Sobkowiak, B. Levänen, M. Sköld,

E. A. Thompson, O. Saher, O. K. Kari, T. Lajunen, E. Sverremark Ekström, C. Nilsson, Y. Ishchenko, T. Malm, M. J. A. Wood, U. F. Power, S. Masich, A. Lindén, J. K. Sandberg, J. Lehtiö, A.-L. Spetz, S. El Andaloussi, *Nat. Commun.* **2019**, *10*, 2331.
[61] M. Hadjidemetriou, Z. Al-Ahmady, K. Kostarelos, *Nanoscale* **2016**, *8*, 6948.
[62] G. La Barbera, A. L. Capriotti, G. Caracciolo, C. Cavaliere, A. Cerrato, C. M. Montone, S. Piovesana, D. Pozzi, E. Quagliarini, A. Laganà, *Talanta* **2020**, *209*, 120487.
[63] J. Müller, D. Prozeller, A. Ghazaryan, M. Kokkinopoulou, V. Mailänder, S. Morsbach, K. Landfester, *Acta Biomater.* **2018**, *71*, 420.
[64] A. J. Chetwynd, W. Zhang, J. A. Thorn, I. Lynch, R. Ramautar, *Small* **2020**, *16*, 2000295.
[65] S. Winzen, S. Schoettler, G. Baier, C. Rosenauer, V. Mailaender, K. Landfester, K. Mohr, *Nanoscale* **2015**, *7*, 2992.
[66] E. Casals, T. Pfaller, A. Duschl, G. J. Oostingh, V. Puntes, *ACS Nano* **2010**, *4*, 3623.
[67] C. Pisani, J.-C. Gaillard, M. Odorico, J. L. Nyalosaso, C. Charnay, Y. Guari, J. Chopineau, J.-M. Devoisselle, J. Armengaud, O. Prat, *Nanoscale* **2017**, *9*, 1840.
[68] J. Piella, N. G. Bastús, V. Puntes, *Bioconjugate Chem.* **2017**, *28*, 88.
[69] R. García-Álvarez, M. Hadjidemetriou, A. Sánchez-Iglesias, L. M. Liz-Marzán, K. Kostarelos, *Nanoscale* **2018**, *10*, 1256.
[70] G. Wang, W. Wang, E. Shangguan, S. Gao, Y. Liu, *Mater. Sci. Eng., C* **2020**, *111*, 110830.
[71] A. M. Clemments, P. Botella, C. C. Landry, *ACS Appl. Mater. Interfaces* **2015**, *7*, 21682.
[72] C. Gräfe, A. Weidner, M. v. d. Lühe, C. Bergemann, F. H. Schacher, J. H. Clement, S. Dutz, *Int. J. Biochem. Cell Biol.* **2016**, *75*, 196.
[73] U. Sakulkhu, M. Mahmoudi, L. Maurizi, G. Coullerez, M. Hofmann-Amtenbrink, M. Vries, M. Motazacker, F. Rezaee, H. Hofmann, *Biomater. Sci.* **2015**, *3*, 265.
[74] W. Lai, Q. Wang, L. Li, Z. Hu, J. Chen, Q. Fang, *Colloids Surf., B* **2017**, *152*, 317.
[75] A. L. Barrán-Berdón, D. Pozzi, G. Caracciolo, A. L. Capriotti, G. Caruso, C. Cavaliere, A. Riccioli, S. Palchetti, A. Laganà, *Langmuir* **2013**, *29*, 6485.
[76] D. Burnand, A. Milosevic, S. Balog, M. Spuch-Calvar, B. Rothen-Rutishauser, J. Dengjel, C. Kinnear, T. L. Moore, A. Petri-Fink, *Small* **2018**, *14*, 1802088.
[77] M. Papi, D. Caputo, V. Palmieri, R. Coppola, S. Palchetti, F. Bugli, C. Martini, L. Digiacomo, D. Pozzi, G. Caracciolo, *Nanoscale* **2017**, *9*, 10327.
[78] G. Stepien, M. Moros, M. Pérez-Hernández, M. Monge, L. Gutiérrez, R. M. Fratila, M. De Las Heras, S. Menao Guillén, J. J. Puente Lanzarote, C. Solans, J. Pardo, J. M. De La Fuente, *ACS Appl. Mater. Interfaces* **2018**, *10*, 4548.
[79] C. C. S. Batista, L. J. C. Albuquerque, A. Jäger, P. Stepánek, F. C. Giacomelli, *Mater. Sci. Eng., C* **2020**, *111*, 110850.
[80] A.-K. Danner, S. Schöttler, E. Alexandrino, S. Hammer, K. Landfester, V. Mailänder, S. Morsbach, H. Frey, F. R. Wurm, *Macromol. Biosci.* **2019**, *19*, 1800468.
[81] K. R. Riley, C. M. Sims, I. T. Wood, D. J. Vanderah, M. L. Walker, *Anal. Bioanal. Chem.* **2018**, *410*, 145.
[82] J. Müller, K. N. Bauer, D. Prozeller, J. Simon, V. Mailänder, F. R. Wurm, S. Winzen, K. Landfester, *Biomaterials* **2017**, *115*, 1.
[83] B. Huang, Z. Yang, S. Fang, Y. Li, Z. Zhong, R. Zheng, J. Zhang, H. Wang, S. Wang, Q. Zou, L. Wu, *Nanoscale* **2020**, *12*, 5834.
[84] J. Müller, J. Simon, P. Rohne, C. Koch-Brandt, V. Mailänder, S. Morsbach, K. Landfester, *Biomacromolecules* **2018**, *19*, 2657.
[85] G. Caracciolo, D. Pozzi, A. L. Capriotti, C. Cavaliere, P. Foglia, H. Amenitsch, A. Laganà, *Langmuir* **2011**, *27*, 15048.
[86] D. H. Jo, J. H. Kim, J. G. Son, K. S. Dan, S. H. Song, T. G. Lee, J. H. Kim, *Biomaterials* **2016**, *109*, 23.
[87] L. K. Müller, J. Simon, C. Rosenauer, V. Mailänder, S. Morsbach, K. Landfester, *Biomacromolecules* **2018**, *19*, 374.
[88] M. Hadjidemetriou, Z. Al-ahmady, M. Buggio, J. Swift, K. Kostarelos, *Biomaterials* **2019**, *188*, 118.
[89] M. Hadjidemetriou, Z. Al-Ahmady, M. Mazza, R. F. Collins, K. Dawson, K. Kostarelos, *ACS Nano* **2015**, *9*, 8142.
[90] M. P. Monopoli, D. Walczyk, A. Campbell, G. Elia, I. Lynch, F. Baldelli Bombelli, K. A. Dawson, *J. Am. Chem. Soc.* **2011**, *133*, 2525.
[91] M. Hadjidemetriou, S. Mcadam, G. Garner, C. Thackeray, D. Knight, D. Smith, Z. Al-Ahmady, M. Mazza, J. Rogan, A. Clamp, K. Kostarelos, *Adv. Mater.* **2019**, *31*, 1803335.
[92] D. T. Jayaram, S. M. Pustulka, R. G. Mannino, W. A. Lam, C. K. Payne, *Biophys. J.* **2018**, *115*, 209.
[93] D. Pozzi, G. Caracciolo, L. Digiacomo, V. Colapicchioni, S. Palchetti, A. L. Capriotti, C. Cavaliere, R. Zenezini Chiozzi, A. Puglisi, A. Laganà, *Nanoscale* **2015**, *7*, 13958.
[94] A. Kumar, E. M. Bicer, A. B. Morgan, P. E. Pfeffer, M. Monopoli, K. A. Dawson, J. Eriksson, K. Edwards, S. Lynham, M. Arno, A. F. Behndig, A. Blomberg, G. Somers, D. Hassall, L. A. Dailey, B. Forbes, I. S. Mudway, *Nanomedicine* **2016**, *12*, 1033.
[95] S. Prakash, R. Deswal, *Plant Physiol. Biochem.* **2020**, *146*, 143.
[96] M. Lundqvist, J. Stigler, T. Cedervall, T. Berggård, M. B. Flanagan, I. Lynch, G. Elia, K. Dawson, *ACS Nano* **2011**, *5*, 7503.
[97] Z. Ma, J. Bai, X. Jiang, *ACS Appl. Mater. Interfaces* **2015**, *7*, 17614.
[98] M. Mahmoudi, M. A. Shokrgozar, S. Behzadi, *Nanoscale* **2013**, *5*, 3240.
[99] A. Weidner, C. Gräfe, M. von der Lühe, H. Remmer, J. H. Clement, D. Eberbeck, F. Ludwig, R. Müller, F. H. Schacher, S. Dutz, *Nanoscale Res. Lett.* **2015**, *10*, 282.
[100] M. Mahmoudi, S. E. Lohse, C. J. Murphy, A. Fathizadeh, A. Montazeri, K. S. Suslick, *Nano Lett.* **2014**, *14*, 6.
[101] U. Martens, D. Böttcher, D. Talbot, U. Bornscheuer, A. Abou-Hassan, M. Delcea, *Nanoscale* **2019**, *11*, 16063.
[102] S. Liu, Z. Wang, X. Jiang, J. Gan, X. Tian, Z. Xing, Y. Yan, J. Chen, J. Zhang, C. Wang, L. Dong, *Biomaterials* **2021**, *265*, 120452.
[103] A. Cox, P. Andreozzi, R. Dal Magro, F. Fiordaliso, A. Corbelli, L. Talamini, C. Chinello, F. Raimondo, F. Magni, M. Tringali, S. Krol, P. J. Silva, F. Stellacci, M. Masserini, F. Re, *ACS Nano* **2018**, *12*, 7292.
[104] M. Qin, J. Zhang, M. Li, D. Yang, D. Liu, S. Song, J. Fu, H. Zhang, W. Dai, X. Wang, Y. Wang, B. He, Q. Zhang, *Theranostics* **2020**, *10*, 1213.
[105] R. R. Arvizo, K. Giri, D. Moyano, O. R. Miranda, B. Madden, D. J. McCormick, R. Bhattacharya, V. M. Rotello, J.-P. Kocher, P. Mukherjee, *PLoS One* **2012**, *7*, e33650.
[106] D. Caputo, M. Papi, R. Coppola, S. Palchetti, L. Digiacomo, G. Caracciolo, D. Pozzi, *Nanoscale* **2017**, *9*, 349.
[107] V. Colapicchioni, M. Tilio, L. Digiacomo, V. Gambini, S. Palchetti, C. Marchini, D. Pozzi, S. Occhipinti, A. Amici, G. Caracciolo, *Int. J. Biochem. Cell Biol.* **2016**, *75*, 180.
[108] A. Kumar, E. M. Bicer, P. Pfeffer, M. P. Monopoli, K. A. Dawson, J. Eriksson, K. Edwards, S. Lynham, M. Arno, A. F. Behndig, A. Blomberg, G. Somers, D. Hassall, L. A. Dailey, B. Forbes, I. Mudway, *Nanomedicine* **2017**, *13*, 2517.
[109] M. Magro, M. Zaccarin, G. Miotto, L. Da Dalt, D. Baratella, P. Fariselli, G. Gabai, F. Vianello, *Anal. Bioanal. Chem.* **2018**, *410*, 2949.
[110] M. Garvas, A. Testen, P. Umek, A. Gloter, T. Koklic, J. Strancar, *PLoS One* **2015**, *10*, e0129577.
[111] T. Miclăuş, C. Beer, J. Chevallier, C. Scavenius, V. E. Bochenkov, J. J. Enghild, D. S. Sutherland, *Nat. Commun.* **2016**, *7*, 11770.
[112] G. Duan, S. Kang, X. Tian, J. A. Garate, L. Zhao, C. Ge, R. Zhou, *Nanoscale* **2015**, *7*, 15214.
[113] Y. Song, H. Wang, L. Zhang, B. Lai, K. Liu, M. Tan, *Food Funct.* **2020**, *11*, 2358.

[114] T. Yoshida, Y. Yoshioka, Y. Morishita, M. Aoyama, S. Tochigi, T. Hirai, K. Tanaka, K. Nagano, H. Kamada, S.-I. Tsunoda, H. Nabeshi, T. Yoshikawa, K. Higashisaka, Y. Tsutsumi, *Nanotechnology* **2015**, *26*, 245101.
[115] D. Chen, N. Parayath, S. Ganesh, W. Wang, M. Amiji, *Nanoscale* **2019**, *11*, 18806.
[116] R. Dal Magro, B. Albertini, S. Beretta, R. Rigolio, E. Donzelli, A. Chiorazzi, M. Ricci, P. Blasi, G. Sancini, *Nanomedicine* **2018**, *14*, 429.
[117] S. Wu, L. Gu, J. Qin, L. Zhang, F. Sun, Z. Liu, Y. Wang, D. Shi, *ACS Appl. Mater. Interfaces* **2020**, *12*, 4193.
[118] J. Mo, Y. Xu, X. Wang, W. Wei, J. Zhao, *Nanoscale* **2020**, *12*, 1742.
[119] J. Simon, L. K. Müller, M. Kokkinopoulou, I. Lieberwirth, S. Morsbach, K. Landfester, V. Mailänder, *Nanoscale* **2018**, *10*, 10731.
[120] F. Giulimondi, L. Digiacomo, D. Pozzi, S. Palchetti, E. Vulpis, A. L. Capriotti, R. Z. Chiozzi, A. Laganà, H. Amenitsch, L. Masuelli, G. Peruzzi, M. Mahmoudi, I. Screpanti, A. Zingoni, G. Caracciolo, *Nat. Commun.* **2019**, *10*, 3686.
[121] S. Shahabi, L. Treccani, R. Dringen, K. Rezwan, *Nanoscale* **2015**, *7*, 16251.
[122] D. Chakraborty, L. Mohan, S. A. Alex, N. Chandrasekaran, A. Mukherjee, *Biomater. Sci.* **2019**, *7*, 63.
[123] E. L. L. Yeo, P. S. P. Thong, K. C. Soo, J. C. Y. Kah, *Nanoscale* **2018**, *10*, 2461.
[124] R. Wu, H. Peng, J.-J. Zhu, L.-P. Jiang, J. Liu, *Front. Chem.* **2020**, *8*, 121.
[125] H.-W. Chen, C.-Y. Huang, S.-Y. Lin, Z.-S. Fang, C.-H. Hsu, J.-C. Lin, Y.-I. Chen, B.-Y. Yao, C.-M. J. Hu, *Biomaterials* **2016**, *106*, 111.
[126] X. Zhang, Y. Liu, S. Gopalakrishnan, L. Castellanos-Garcia, G. Li, M. Malassiné, I. Uddin, R. Huang, D. C. Luther, R. W. Vachet, V. M. Rotello, *ACS Nano* **2020**, *14*, 4767.
[127] X. Zeng, J. Sun, S. Li, J. Shi, H. Gao, W. Sun Leong, Y. Wu, M. Li, C. Liu, P. Li, J. Kong, Y.-Z. Wu, G. Nie, Y. Fu, G. Zhang, *Nat. Commun.* **2020**, *11*, 567.
[128] J. Yang, B. Wang, Y. You, W.-J. Chang, K. Tang, Y.-C. Wang, W. Zhang, F. Ding, S. Gunasekaran, *Nanoscale* **2017**, *9*, 17758.
[129] Y. Zhang, J. Hao, X. Xu, X. Chen, J. Wang, *Anal. Chem.* **2020**, *92*, 2080.
[130] K. P. Chan, Y. Gao, J. X. Goh, D. Susanti, E. L. L. Yeo, S.-H. Chao, J. C. Y. Kah, *ACS Appl. Mater. Interfaces* **2017**, *9*, 10408.
[131] J. O'Brien, S.-H. Lee, S. Onogi, K. J. Shea, *J. Am. Chem. Soc.* **2016**, *138*, 16604.
[132] X. Xu, X. Mao, Y. Wang, D. Li, Z. Du, W. Wu, L. Jiang, J. Yang, J. Li, *Int. J. Biol. Macromol.* **2018**, *116*, 492.
[133] R. L. Pinals, D. Yang, A. Lui, W. Cao, M. P. Landry, *J. Am. Chem. Soc.* **2020**, *142*, 1254.
[134] K. Strojan, A. Leonardi, V. B. Bregar, I. Križaj, J. Svete, M. Pavlin, *PLoS One* **2017**, *12*, e0169552.
[135] Y. Hayashi, T. Miclaus, C. Scavenius, K. Kwiatkowska, A. Sobota, P. Engelmann, J. J. Scott-Fordsmand, J. J. Enghild, D. S. Sutherland, *Environ. Sci. Technol.* **2013**, *47*, 14367.
[136] S. Ritz, S. Schöttler, N. Kotman, G. Baier, A. Musyanovych, J. Kuharev, K. Landfester, H. Schild, O. Jahn, S. Tenzer, V. Mailänder, *Biomacromolecules* **2015**, *16*, 1311.
[137] R. Aebersold, M. Mann, *Nature* **2003**, *422*, 198.
[138] F. Bertoli, D. Garry, M. P. Monopoli, A. Salvati, K. A. Dawson, *ACS Nano* **2016**, *10*, 10471.
[139] A. C. G. Weiss, K. Krüger, Q. A. Besford, M. Schlenk, K. Kempe, S. Förster, F. Caruso, *ACS Appl. Mater. Interfaces* **2019**, *11*, 2459.
[140] X. Lin, Q. Pan, Y. He, *Nanoscale* **2019**, *11*, 18367.
[141] N. Feiner-Gracia, M. Beck, S. Pujals, S. Tosi, T. Mandal, C. Buske, M. Linden, L. Albertazzi, *Small* **2017**, *13*, 1701631.
[142] A. O. Khan, A. Di Maio, E. J. Guggenheim, A. J. Chetwynd, D. Pencross, S. Tang, M.-F. A. Belinga-Desaunay, S. G. Thomas, J. Z. Rappoport, I. Lynch, *Nanomaterials* **2020**, *10*, 401.
[143] M. Plaza-Oliver, M. J. Santander-Ortega, L. Castro-Vázquez, V. Rodríguez-Robledo, J. González-Fuentes, P. Marcos, M. V Lozano, M. M. Arroyo-Jiménez, *Colloids Surf., B* **2020**, *186*, 110740.
[144] M. Kokkinopoulou, J. Simon, K. Landfester, V. Mailänder, I. Lieberwirth, *Nanoscale* **2017**, *9*, 8858.
[145] S. Lara, F. Alnasser, E. Polo, D. Garry, M. C. Lo Giudice, D. R. Hristov, L. Rocks, A. Salvati, Y. Yan, K. A. Dawson, *ACS Nano* **2017**, *11*, 1884.
[146] S. Sheibani, K. Basu, A. Farnudi, A. Ashkarran, M. Ichikawa, J. F. Presley, K. H. Bui, M. R. Ejtehadi, H. Vali, M. Mahmoudi, *Nat. Commun.* **2021**, *12*, 573.
[147] M.-M. Yin, W.-Q. Chen, Y.-Q. Lu, J.-Y. Han, Y. Liu, F.-L. Jiang, *Nanoscale* **2020**, *12*, 4573.
[148] Kenry, T. Yeo, P. N. Manghnani, E. Middha, Y. Pan, H. Chen, C. T. Lim, B. Liu, *ACS Nano* **2020**, *14*, 4509.
[149] Q. Dai, Y. Yan, C.-S. Ang, K. Kempe, M. M. J. Kamphuis, S. J. Dodds, F. Caruso, *ACS Nano* **2015**, *9*, 2876.
[150] C. Corbo, R. Molinaro, F. Taraballi, N. E. Toledano Furman, K. A. Hartman, M. B. Sherman, E. De Rosa, D. K. Kirui, F. Salvatore, E. Tasciotti, *ACS Nano* **2017**, *11*, 3262.
[151] A. L. Lira, R. S. Ferreira, R. J. S. Torquato, H. Zhao, M. L. V. Oliva, S. A. Hassan, P. Schuck, A. A. Sousa, *Nanoscale* **2018**, *10*, 3235.
[152] F. E. Galdino, A. S. Picco, M. L. Sforca, M. B. Cardoso, W. Loh, *Colloids Surf., B* **2020**, *186*, 110677.
[153] M. Raoufi, M. J. Hajipour, S. M. Kamali Shahri, I. Schoen, U. Linn, M. Mahmoudi, *Nanoscale* **2018**, *10*, 1228.
[154] Z.-T. Cao, L.-Q. Gan, W. Jiang, J.-L. Wang, H.-B. Zhang, Y. Zhang, Y. Wang, X. Yang, M. Xiong, J. Wang, *ACS Nano* **2020**, *14*, 3563.
[155] O. Vilanova, J. J. Mittag, P. M. Kelly, S. Milani, K. A. Dawson, J. O. Rädler, G. Franzese, *ACS Nano* **2016**, *10*, 10842.
[156] M. Carril, D. Padro, P. delPino, C. Carrillo-Carrion, M. Gallego, W. J. Parak, *Nat. Commun.* **2017**, *8*, 1542.
[157] S. Motta, V. Rondelli, L. Cantu, E. Del Favero, M. Aureli, D. Pozzi, G. Caracciolo, P. Brocca, *Colloids Surf., B* **2016**, *141*, 170.
[158] L. Marichal, G. Giraudon-Colas, F. Cousin, A. Thill, J. Labarre, Y. Boulard, J.-C. Aude, S. Pin, J. P. Renault, *Langmuir* **2019**, *35*, 10831.
[159] D. Di Silvio, M. Maccarini, R. Parker, A. Mackie, G. Fragneto, F. Baldelli Bombelli, *J. Colloid Interface Sci.* **2017**, *504*, 741.
[160] L. Wang, J. Li, J. Pan, X. Jiang, Y. Ji, Y. Li, Y. Qu, Y. Zhao, X. Wu, C. Chen, *J. Am. Chem. Soc.* **2013**, *135*, 17359.
[161] C. Minelli, A. Sikora, R. Garcia-Diez, K. Sparnacci, C. Gollwitzer, M. Krumrey, A. G. Shard, *Anal. Methods* **2018**, *10*, 1725.
[162] D. J. O'Connell, F. B. Bombelli, A. S. Pitek, M. P. Monopoli, D. J. Cahill, K. A. Dawson, *Nanoscale* **2015**, *7*, 15268.
[163] O. Koshkina, T. Lang, R. Thiermann, D. Docter, R. H. Stauber, C. Secker, H. Schlaad, S. Weidner, B. Mohr, M. Maskos, A. Bertin, *Langmuir* **2015**, *31*, 8873.
[164] J. Ashby, S. Pan, W. Zhong, *ACS Appl. Mater. Interfaces* **2014**, *6*, 15412.
[165] C. Weber, J. Simon, V. Mailänder, S. Morsbach, K. Landfester, *Acta Biomater.* **2018**, *76*, 217.
[166] C. V. Raman, K. S. Krishnan, *Nature* **1928**, *121*, 501.
[167] G. S. Bumbrah, R. M. Sharma, *Egypt. J. Forensic Sci.* **2016**, *6*, 209.
[168] H. J. Butler, L. Ashton, B. Bird, G. Cinque, K. Curtis, J. Dorney, K. Esmonde-White, N. J. Fullwood, B. Gardner, P. L. Martin-Hirsch, M. J. Walsh, M. R. Mcainsh, N. Stone, F. L. Martin, *Nat. Protoc.* **2016**, *11*, 664.
[169] Z. Movasaghi, S. Rehman, I. U. Rehman, *Appl. Spectrosc. Rev.* **2007**, *42*, 493.

[170] G. Hiremath, A. Locke, A. Sivakumar, G. Thomas, A. Mahadevan-Jansen, *J. Gastroenterol. Hepatol.* **2019**, *34*, 1911.
[171] M. Fleischmann, P. J. Hendra, A. J. McQuillan, *Chem. Phys. Lett.* **1974**, *26*, 163.
[172] R. R. Jones, D. C. Hooper, L. Zhang, D. Wolverson, V. K. Valev, *Nanoscale Res. Lett.* **2019**, *14*, 231.
[173] C. Chen, W. Liu, S. Tian, T. Hong, *Sensors* **2019**, *19*, 1712.
[174] D. Cam, K. Keseroglu, M. Kahraman, F. Sahin, M. Culha, *J. Raman Spectrosc.* **2010**, *41*, 484.
[175] J. Liu, M. Jalali, S. Mahshid, S. Wachsmann-Hogiu, *Analyst* **2020**, *145*, 364.
[176] L. Mikac, M. Ivanda, M. Gotić, et. al., *J. Nanopart Res.* **2014**, *16*, 2748.
[177] S. Hong, X. Li, *J. Nanomater.* **2013**, *2013*, 9.
[178] K. D. Alexander, K. Skinner, S. Zhang, H. Wei, R. Lopez, *Nano Lett.* **2010**, *10*, 4488.
[179] J. Krajczewski, A. Michałowska, A. Kudelski, *Spectrochim. Acta, Part A* **2020**, *225*, 117469.
[180] L. A. Osminkina, O. Žukovskaja, S. N. Agafilushkina, E. Kaniukov, O. Stranik, K. A. Gonchar, D. Yakimchuk, V. Bundyukova, D. A. Chermoshentsev, S. A. Dyakov, N. A. Gippius, K. Weber, J. Popp, D. Cialla–May, V. Sivakov, *Appl. Surf. Sci.* **2020**, *507*, 144989.
[181] D. Huang, J. Zhao, M. Wang, S. Zhu, *Food Control* **2020**, *108*, 106835.
[182] S. Lee, H. D. Song, Y. I. Yang, G.-P. Kim, I. Choi, J. Yi, *Chem. Commun.* **2015**, *51*, 213.
[183] B. Prats-Mateu, N. Gierlinger, *Microsc. Res. Tech.* **2017**, *80*, 30.
[184] A. Sharikova, Z. I. Foraida, L. Sfakis, L. Peerzada, M. Larsen, J. Castracane, A. Khmaladze, *Spectrochim. Acta, Part A* **2020**, *227*, 117670.
[185] L. Sfakis, A. Sharikova, D. Tuschel, F. X. Costa, M. Larsen, A. Khmaladze, J. Castracane, *Biomed. Opt. Express* **2017**, *8*, 1025.
[186] B. Prats Mateu, M. T. Hauser, A. Heredia, N. Gierlinger, *Front. Chem.* **2016**, *4*, 10.
[187] P. J. Caspers, G. W. Lucassen, G. J. Puppels, *Biophys. J.* **2003**, *85*, 572.
[188] K. Klein, A. M. Gigler, T. Aschenbrenner, R. Monetti, W. Bunk, F. Jamitzky, G. Morfill, R. W. Stark, J. Schlegel, *Biophys. J.* **2012**, *102*, 360.
[189] I. Estrela-Lopis, G. Romero, E. Rojas, S. E. Moya, E. Donath, *J. Phys.: Conf. Ser.* **2011**, *304*, 012017.
[190] N. Everall, *Spectroscopy* **2004**, *19*, 22.
[191] M. Offroy, M. Moreau, S. Sobanska, P. Milanfar, L. Duponchel, *Sci. Rep.* **2015**, *5*, 12303.
[192] F. Hu, L. Shi, W. Min, *Nat. Methods* **2019**, *16*, 830.
[193] R. M. Molina, N. V Konduru, P. M. Queiroz, B. Figueroa, D. Fu, L. Ma-Hock, S. Groeters, D. Schaudien, J. D. Brain, *Sci. Rep.* **2019**, *9*, 8163.
[194] S. Vanden-Hehir, S. A. Cairns, M. Lee, L. Zoupi, M. P. Shaver, V. G. Brunton, A. Williams, A. N. Hulme, *Biomacromolecules* **2019**, *20*, 4008.
[195] W. J. Tipping, M. Lee, A. Serrels, V. G. Brunton, A. N. Hulme, *Chem. Sci.* **2017**, *8*, 5606.
[196] N. A. Belsey, N. L. Garrett, L. R. Contreras-Rojas, A. J. Pickup-Gerlaugh, G. J. Price, J. Moger, R. H. Guy, *J. Controlled Release* **2014**, *174*, 37.
[197] M. M. Gaschler, F. Hu, H. Feng, A. Linkermann, W. Min, B. R. Stockwell, *ACS Chem. Biol.* **2018**, *13*, 1013.
[198] S. Gomes da Costa, A. Richter, U. Schmidt, S. Breuninger, O. Hollricher, *Morphologie* **2019**, *103*, 11.
[199] J. W. Kang, Y. S. Park, H. Chang, W. Lee, S. P. Singh, W. Choi, L. H. Galindo, R. R. Dasari, S. H. Nam, J. Park, P. T. C. So, *Sci. Adv.* **2020**, *6*, eaay5206.
[200] W. C. Zúñiga, V. Jones, S. M. Anderson, A. Echevarria, N. L. Miller, C. Stashko, D. Schmolze, P. D. Cha, R. Kothari, Y. Fong, M. C. Storrie-Lombardi, *Sci. Rep.* **2019**, *9*, 14639.
[201] M. Shao, L. Lu, H. Wang, S. Luo, D. D. D. Ma, *Microchim. Acta* **2009**, *164*, 157.
[202] J. Ni, R. J. Lipert, G. B. Dawson, M. D. Porter, *Anal. Chem.* **1999**, *71*, 4903.
[203] M. Iosin, F. Toderas, P. L. Baldeck, S. Astilean, *J. Mol. Struct.* **2009**, *924–926*, 196.
[204] S. Grass, L. Treuel, *J. Nanopart. Res.* **2014**, *16*, 2254.
[205] G. P. Szekeres, J. Kneipp, *Analyst* **2018**, *143*, 6061.
[206] M. Gambucci, P. L. Gentili, P. Sassi, L. Latterini, *Soft Matter* **2019**, *15*, 6571.
[207] O. Neumann, D. Zhang, F. Tam, S. Lal, P. Wittung-Stafshede, N. J. Halas, *Anal. Chem.* **2009**, *81*, 10002.
[208] R. Dekhili, K. Cherni, H. Liu, X. Li, N. Djaker, J. Spadavecchia, *ACS Omega* **2020**, *5*, 13851.
[209] T. Barkhade, A. Phatangare, S. Dahiwale, S. K. Mahapatra, I. Banerjee, *Surf. Interface Anal.* **2019**, *51*, 894.
[210] S. Barkur, J. Lukose, S. Chidangil, *ACS Omega* **2020**, *5*, 1439.
[211] S. Vanden-Hehir, W. J. Tipping, M. Lee, V. G. Brunton, A. Williams, A. N. Hulme, *Nanomaterials* **2019**, *9*, 341.
[212] T. Cedervall, I. Lynch, S. Lindman, T. Berggård, E. Thulin, H. Nilsson, K. A. Dawson, S. Linse, *Proc. Natl. Acad. Sci. USA* **2007**, *104*, 2050 LP.
[213] K. Chaudhary, K. Kumar, P. Venkatesu, D. T. Masram, *Nanoscale Adv.* **2020**, *2*, 2146.
[214] G. P. Szekeres, J. Kneipp, *Front. Chem.* **2019**, *7*, 30.
[215] G. P. Szekeres, M. Montes-Bayón, J. Bettmer, J. Kneipp, *Anal. Chem.* **2020**, *92*, 8553.
[216] S. Sloan-Dennison, M. R. Bevins, B. T. Scarpitti, V. K. Sauvé, Z. D. Schultz, *Analyst* **2019**, *144*, 5538.

Matteo Battaglini received his Ph.D. in biorobotics in 2020 from Scuola Superiore Sant'Anna (Pisa, Italy) working on the synthesis and testing of nanomaterials for biomedical applications, besides on the establishment of advanced in vitro models. He is currently a post-doctoral fellow working in the Smart Bio-Interfaces Research Line of the Italian Institute of Technology (Pontedera, Italy). His research interests include the design, the fabrication, and the testing of smart nanomaterials for human healthcare, and the development of innovative in vitro models of biological structures.

Melike Belenli Gümüş is a second-year Ph.D. student at the joint program between The Biorobotics Institute of the Sant'Anna School of Advanced Studies and the Italian Institute of Technology (Pontedera, Italy). Her research interests include smart nanomaterials for targeted drug delivery and Raman spectroscopy applications at the nano–biointerface.

Gianni Ciofani, Ph.D., is the research director at the Italian Institute of Technology, where he is the principal investigator of the Smart Bio-Interfaces Research Line and Coordinator of the Center for Materials Interfaces (Pontedera, Italy). His main research interests are in the field of smart nanomaterials for nanomedicine, bio/nonbiointeractions, and biology in altered gravity conditions.